



Cite this: *Lab Chip*, 2025, **25**, 3060



## Advances in nanoparticle synthesis assisted by microfluidics

Muhammad Mubashar Saeed, <sup>a,b,c,d</sup> Eadaoin Carthy, <sup>b,c,d</sup>  
 Nicholas Dunne <sup>b,c,e,f,g,h,i,j,k</sup> and David Kinahan <sup>b,c,d</sup>

The synthesis of nanoparticles (NPs) has garnered significant interest due to their wide-ranging applications across various emerging industries, including pharmaceuticals, electronics, food engineering, agriculture, wastewater management, and medicine. Research efforts have focused on controlling key NP characteristics, such as size, polydispersity, zeta potential, drug release, and encapsulation efficiency, to meet the demands of these applications. In this review, we explore how microfluidics offers a superior alternative to conventional physical, chemical, and biological synthesis methods. We discuss various microfluidic NP manufacturing strategies, broadly classified into passive and active methods. Active methods utilise external energy sources, such as thermal, electrical, electromagnetic, and acoustic inputs. In contrast, passive methods do not use external energy sources and instead rely on techniques like hydrodynamic flow focusing, vortex generation, droplet generation, and chaotic advection. We also highlight the challenges associated with NP synthesis in microfluidic devices. Finally, we examine the potential of integrating microfluidics with machine learning algorithms to develop “intelligent microfluidics” for NP synthesis.

Received 25th February 2025,  
 Accepted 6th May 2025

DOI: 10.1039/d5lc00194c

rsc.li/loc

### 1. Introduction

The design and synthesis of nanoparticles (NPs) are active and innovative research areas, garnering significant attention from numerous academic groups.<sup>1–3</sup> NPs have gained prominence due to their unique and tuneable properties,<sup>4</sup> including thermal and electrical conductivity,<sup>5,6</sup> melting point,<sup>7,8</sup> and wettability,<sup>9</sup> along with magnetic,<sup>10</sup> catalytic,<sup>11</sup> and optical properties,<sup>12</sup> such as light absorption<sup>13</sup> and scattering.<sup>14</sup>

Traditionally, NPs are defined as materials ranging from 1 to 1000 nm in length in at least one dimension;<sup>15</sup> however, the preferable diameter range is between 1 and 100 nm.<sup>16</sup> The human body consists of nanostructures that play critical roles in body functionality. Therefore, artificially synthesised NPs that can interact with these nanostructures have great potential for applications in biotechnology and biomedical engineering. For example some carbon-based NPs are being used for antimicrobial activities.<sup>17</sup> Lipid-based NPs are being employed for several drug delivery applications.<sup>18</sup>

Several research groups have reviewed different aspects of NP synthesis<sup>19–22</sup> including reviews on microfluidics-based synthesis.<sup>18,23–27</sup> Building on these reviews, this paper provides a comprehensive overview of NP synthesis using microfluidic devices utilizing different active and passive approaches. Section I introduces the fundamentals of NP technology, as well as focuses on their potential applications in medicines. Section II discusses critical factors in assessing NP performance in biomedical contexts. Section III examines the advantages and limitations of conventional NP synthesis and sorting methods, and section IV provides an in-depth discussion of microfluidic-based NP synthesis.

### 2. Nanoparticle technology

Nanoparticles can be applied to a diverse range of innovative applications, such as smart drug delivery systems, solar cells and environmental sensors. NPs have applications in

<sup>a</sup> ML-Labs Centre for Research Training, Dublin City University, Ireland.

E-mail: muhammad.saeed3@mail.dcu.ie

<sup>b</sup> School of Mechanical and Manufacturing Engineering, Dublin City University, Ireland

<sup>c</sup> Biodesign Europe, Dublin City University, Ireland

<sup>d</sup> RAPID Institute, Dublin City University, Ireland

<sup>e</sup> Centre for Medical Engineering Research, School of Mechanical and Manufacturing Engineering, Dublin City University, Dublin, Ireland

<sup>f</sup> Advanced Manufacturing Research Centre (I-Form), School of Mechanical and Manufacturing Engineering, Dublin City University, Dublin, Ireland

<sup>g</sup> SFI Research Centre for Medical Devices (CÚRAM), University of Galway, Galway, Ireland

<sup>h</sup> Advanced Materials and Bioengineering Research Centre (AMBER), Trinity College Dublin, Dublin, Ireland

<sup>i</sup> School of Pharmacy, McClay Research Centre, Medical Biology Centre, Queen's University Belfast, Belfast, UK

<sup>j</sup> Department of Mechanical and Manufacturing Engineering, School of Engineering, Trinity College Dublin, Dublin, Ireland

<sup>k</sup> Trinity Centre for Biomedical Engineering, Trinity Biomedical Sciences Institute, Trinity College Dublin, Dublin, Ireland

# Advanced Applications of Nanoparticles in Different areas

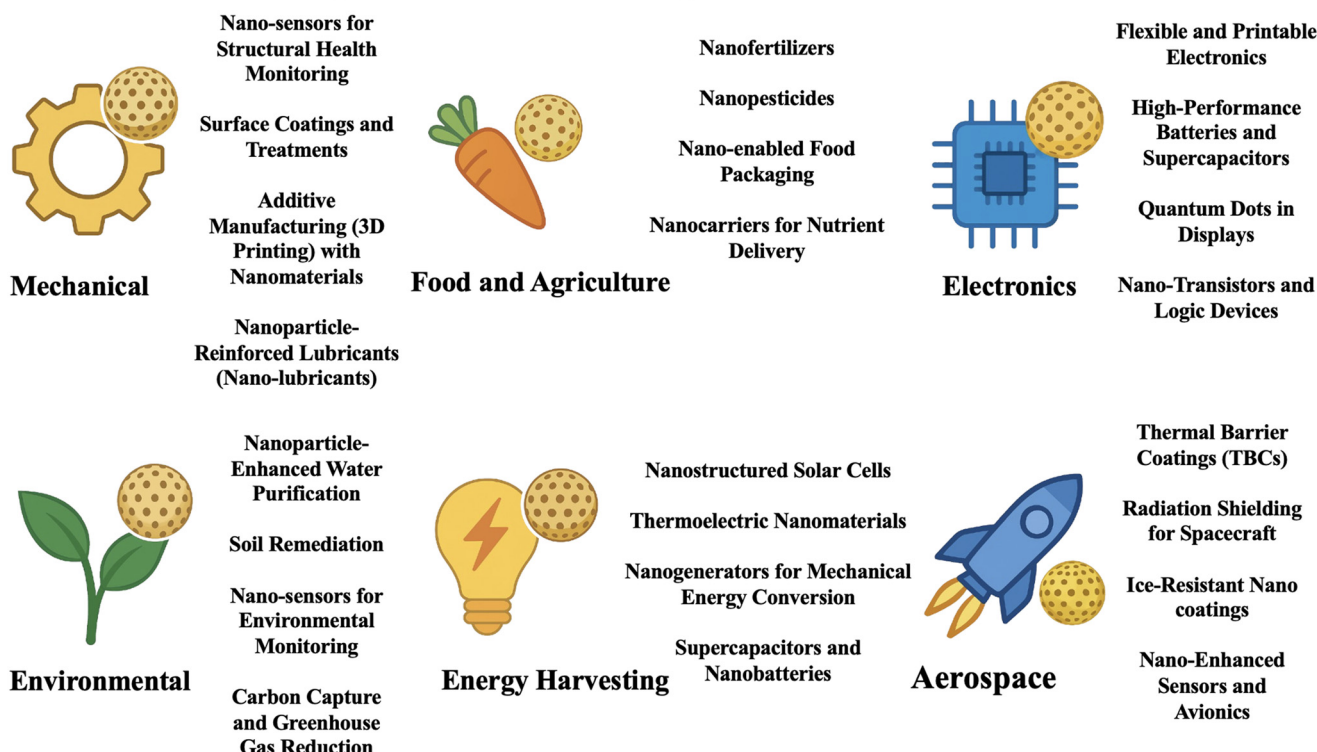


Fig. 1 Diverse innovative applications of NPs in contemporary research fields.

biomedical sciences,<sup>28</sup> as well as in mechanical,<sup>29</sup> food,<sup>30</sup> electronics,<sup>31</sup> environmental,<sup>32,33</sup> energy harvesting<sup>34</sup> and aerospace industry.<sup>35</sup> Different types of innovative applications of nanoparticles (NPs) can be seen in Fig. 1.

Due to the excellent mechanical properties that NPs can offer, they have many applications in coating,<sup>36,37</sup> lubricants,<sup>38</sup> and adhesives.<sup>39</sup> Zirconium carbide (ZrC) NPs have been employed in epoxy-based nanocomposite coatings, demonstrating enhanced mechanical strength and improved corrosion resistance for industrial applications.<sup>40</sup> NPs have also proved useful in increasing the mechanical and thermal properties of fiber reinforced polymer composites.<sup>41</sup> The performance of metals and polymer matrices also improved by embedding NPs in them.<sup>42</sup> NP technology based on alumina, titania and carbon has laid the foundation for the development of desirable coatings.<sup>43–45</sup>

NPs have revolutionized the food industry in various ways.<sup>46</sup> Silver (Ag), titanium dioxide (TiO<sub>2</sub>), and zinc oxide (ZnO) NPs have been employed in the food packaging industry.<sup>47,48</sup> Nanofilms in the form of edible coatings also came up as an innovative strategy to extend the shelf life of perishable products and reduce food waste.<sup>49</sup> NPs have also demonstrated potential applications in the field of electronics.<sup>50,51</sup> Copper (Cu) and Ag NPs have been employed to make high-performance conductive inks for modern electronic chips<sup>52</sup> and flexible printed electronic devices.<sup>53</sup> ZnO NPs have been employed for enhancing electron transport and reducing trap density in P3HT-based hybrid

thin-film transistors, leading to improved carrier mobility, threshold voltage, and potential use in low-cost non-volatile memory and sensing applications.<sup>54</sup> Graphene-based ZnO NPs have been employed for developing thermal smart components with tunable thermal resistance, enabling efficient temperature regulation and energy conservation, showing strong potential for integration into thermal management systems in electronics, spacecraft, and power batteries.<sup>55</sup> NPs also play a vital environmental role in a variety of ways.<sup>56</sup> NPs have been employed for the mitigation of greenhouse gas emissions because of their ability to adsorb CO<sub>2</sub> from industrial processes.<sup>57</sup>

NPs can also contribute to emerging technology areas such as energy harvesting.<sup>34</sup> Zinc ferrite (ZnFe<sub>2</sub>O<sub>4</sub>) NPs have been employed in wearable nanogenerators as self-powered sensors.<sup>58</sup> They can also be used to store energy at the nanoscale level.<sup>34</sup> Silicon (Si) NPs have also been successfully utilized for improving the energy storage performance of lithium ion batteries.<sup>59</sup>

## 2.1. Nanoparticle technology in medicine

NPs have a wide range of applications in the biomedical and pharmaceutical industry, including diagnostics,<sup>60</sup> magnetic resonance imaging (MRI),<sup>61</sup> and drug<sup>62,63</sup> and gene delivery.<sup>64,65</sup> In Fig. 2, different modern applications of NPs are summarised. NPs enable diagnostics at a precise level, even at the single-cell and single-molecule levels. NPs



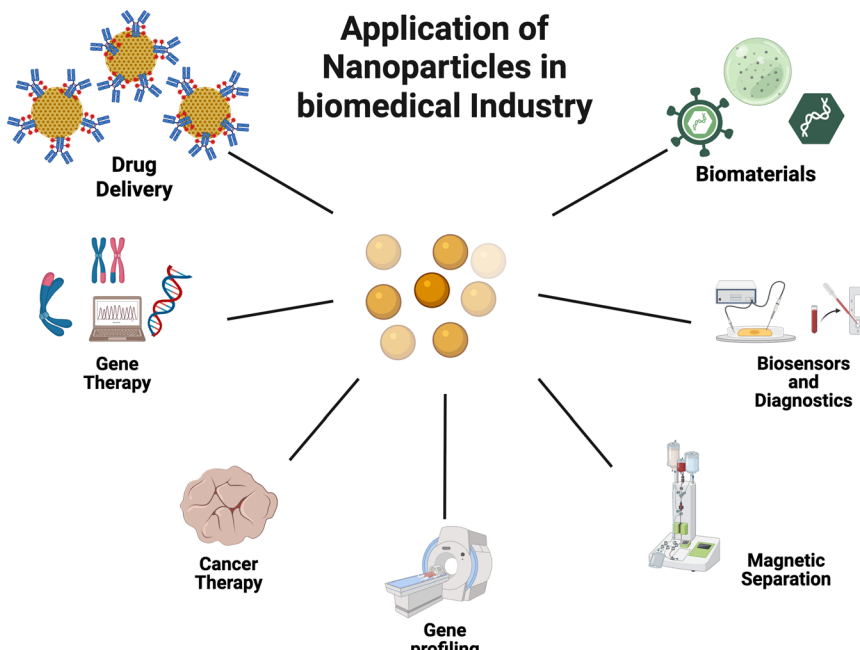


Fig. 2 The expanding role of NPs in biomedical applications and industry that is revolutionising healthcare.

have shown very successful results for diagnosis and treatment of different type of cancers including breast and pancreatic cancer.<sup>60,66,67</sup> Diagnosis and treatment applications of NPs have been recently expanded to bone tumor<sup>68</sup> and atherosclerosis treatment.<sup>69</sup> Magnetic NPs have been used for enhancing MRI imaging as contrast agents due to their unique magnetic and physicochemical properties.<sup>70</sup> Positively charged ZnFe<sub>2</sub>O NPs demonstrated superior MRI efficacy due to enhanced macrophage affinity, offering improved diagnosis of carotid atherosclerosis.<sup>71</sup> Lipid-based NPs,<sup>72</sup> peptide-based NPs,<sup>73</sup> carbon nanotubes<sup>74</sup> and inorganic NPs<sup>75</sup> have brought the recent advancements in smart drug delivery systems. Using NP technology for drug delivery has a range of advantages, such as improved biocompatibility, stability, precise targeting and enhanced biocompatibility.<sup>76</sup> In cancer treatment, NPs have demonstrated greater efficacy and reduced side effects compared to conventional chemotherapeutic medicines. They can deliver drugs with high precision within desired dose parameters and release profiles, as well as protect drugs from degradation, thereby enabling successful transport to the target.<sup>77,78</sup> NPs have also shown potential for use in HIV therapy.<sup>79</sup> The anti-viral drug Nevirapine, which is used for AIDS treatment, can be efficiently delivered using cellulose acetate butyrate (CAB) NPs.<sup>80</sup> Additionally, dietary supplements can be made more effective through delivery *via* NPs.<sup>81,82</sup> Therapeutics can be delivered using four methods: (1) dissolution, (2) encapsulation, (3) entrapment, or (4) attaching to a NP.<sup>83</sup> Nanocapsules, which are reservoir-type devices, consist of a polymer surrounding a cavity where the drug can be contained. In contrast, nanospheres, which are matrix-type

nanodevices, have the drug uniformly dispersed throughout the structure.<sup>84,85</sup>

While liposomes are commonly used as a drug delivery mechanism, they have drawbacks such as low drug encapsulation efficiency, poor stability in drug loading, and swift leakage of water-soluble components.<sup>86</sup> NPs offer an alternative that can mitigate these issues, providing specific advantages in terms of drug loading stability and controlled release at the target site.<sup>87</sup> Research on NP-based drug delivery systems focuses on targeted drug delivery while reducing toxicity. Fig. 3 illustrates the application of NPs in a smart drug delivery system. The major challenges in NP synthesis involve controlling particle size, surface characteristics, zeta potential, and the capacity for drug loading and release.<sup>88</sup>

### 3. Assessing the performance of nanoparticles in drug delivery systems and other biomedical applications

Various physical and chemical characteristics of NPs determine their suitability across diverse applications. In the biomedical field, particle size and surface properties significantly impact the effectiveness of NPs. For smart drug delivery systems utilising NPs, as shown in Fig. 3, factors such as drug loading and release capacity, stability within the body, biocompatibility, targeting ability, and therapeutic efficacy are essential. These factors are in addition to typical considerations like size, shape, and surface properties. This section highlights five critical factors that significantly influence NP performance: size, shape, surface properties, drug loading, and drug release.



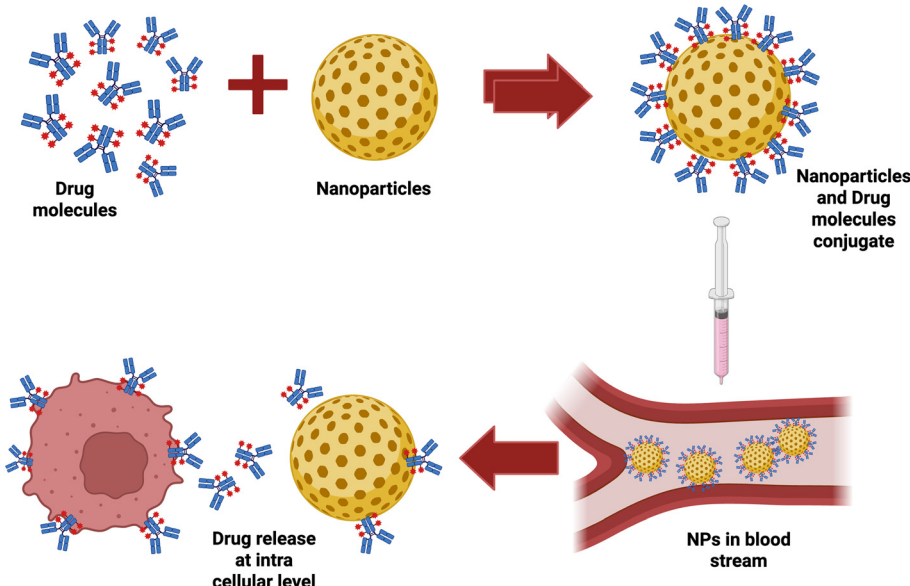


Fig. 3 Schematic representation of an NP-driven drug delivery system for an advanced therapeutics application.

### 3.1. Particle size

The targeting ability and intercellular delivery of drugs in NP-based drug delivery systems depend highly on the NP size and the homogeneity of their size distribution.<sup>89</sup> Particle size plays a pivotal role in determining the drug encapsulation and release efficiency,<sup>90</sup> as well as their stability.<sup>91</sup> Numerous studies have shown that smaller NPs are advantageous for drug release because they can target a wider range of cancer cells and exhibit a higher intercellular uptake compared to larger NPs.<sup>92</sup> The smaller NP size also leads to faster drug release, while larger NPs provide a larger surface area for phagocytosis.<sup>93</sup> However, larger NP can conjugate to a higher volume of drugs due to the larger surface area.

Experimental verification using the Caco-2 cell line<sup>94</sup> has shown that NPs with an average size of 100 nm can exhibit a two-three-fold improvement in drug uptake compared to particles that are 1  $\mu\text{m}$  and a six-fold increase in drug uptake than particles of 10  $\mu\text{m}$  size.<sup>95</sup> The major risk associated with the small size of NPs is their tendency to aggregate during storage and transportation.<sup>96</sup> NPs with a particle size ranging from 2 nm to 100 nm can affect cellular signalling processes. NPs with sizes ranging from 40 nm to 50 nm have been shown to have the greatest effect, especially inducing membrane receptors to down-regulate expression levels. Thus, these NPs can alter downstream signalling and cellular responses in breast cancer cells.<sup>97</sup> The size of NPs can also induce phagocytosis, where NPs with a size greater than 200 nm are targeted by the body's lymphatic system and ingested, unlike relatively smaller size NPs.<sup>98</sup>

### 3.2. Nanoparticle morphology

NP morphology or shape also has a significant impact on their utilisation as a drug delivery agent. Different important

factors, such as cellular uptake, circulation time and biodistribution, targeting efficiency and immune evasion, are directly connected with NP morphology.

Investigation on the crucial role of NP morphology and surface chemistry in drug delivery effectiveness, focusing on ocular applications, has been performed. It has been found that the performance of biodegradable block copolymer NPs in cell uptake, drug release, and diffusion significantly depended on their shape and surface chemistry, with high aspect ratio NPs showing enhanced properties.<sup>99</sup> In another study on understanding the impact of NP shape on cellular transport and drug release, using pair correlation microscopy, it was discovered that different polymeric-shaped NPs—namely, micelles, vesicles, rods, and worms with identical surface chemistries—navigated cellular barriers at varying rates, thus determining the drug release site. It was found that rods and worms, unlike micelles and vesicles, could passively diffuse into the nucleus. Enhancing nuclear access with a nuclear localisation signal increased the cytotoxicity of doxorubicin by enabling more drug release inside the nucleus, affirming the importance of the nuclear envelope as a critical barrier in drug delivery.<sup>100</sup>

### 3.3. Surface properties

Improving the surface properties of NPs can impact their performance and stability *in vivo* for various reasons. When administrated intravenously, NPs are recognised by the immune system, and phagocytes in circulation start clearing them through phagocytosis.<sup>101</sup> To achieve effective targeted drug delivery, it is important to minimise the opsonisation and prolong the circulation of NPs in the bloodstream. Opsonisation refers to the attachment of opsonin protein on the surface of NPs,<sup>102</sup> which helps the body's homeostasis

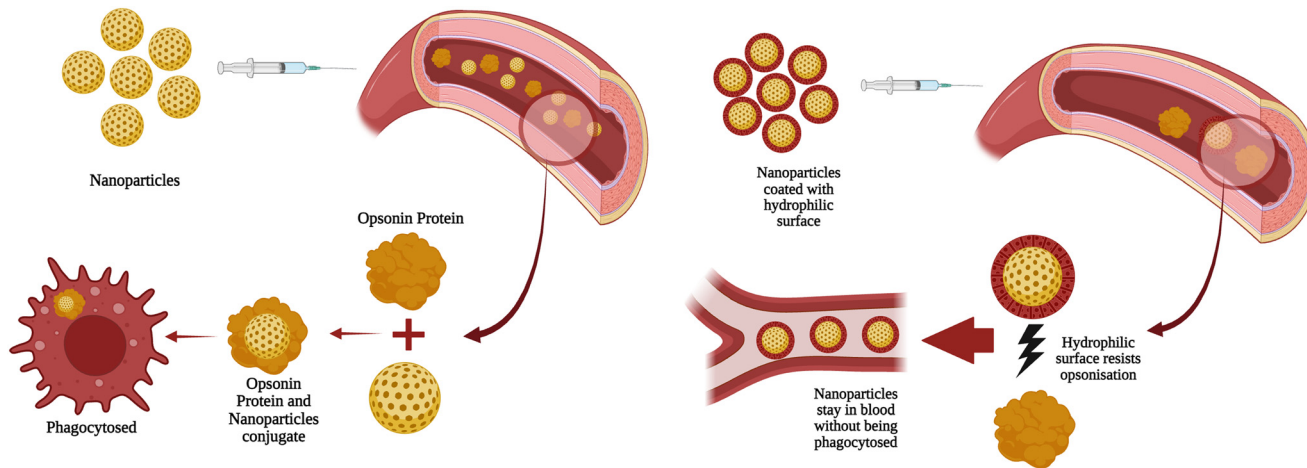


**Fig. 4** a Schematic depiction of the opsonization process that leads to phagocytosis, b: schematic illustration of the significant role of hydrophilic coating in enhancing biocompatibility.

system detect and clear NPs.<sup>103</sup> Fig. 4a illustrates the schematic depiction of the opsonisation-based immune response of the human body. Different techniques can be used to achieve this, including coating the NPs with a hydrophilic polymer or surfactant.<sup>104,105</sup> Fig. 4b defines how hydrophilic coating helps in the biocompatibility of the NPs. Another approach is to use some capping agent for sustained and targeted drug delivery. In this case, NPs are synthesised with biodegradable copolymers and hydrophilic components,<sup>106</sup> such as polyethylene oxide,<sup>107</sup> polyethylene glycol (PEG),<sup>108</sup> polysorbate,<sup>109</sup> and poloxamer.<sup>110</sup>

The zeta potential is the primary measurement associated with the surface charge properties of NPs.<sup>111</sup> The surface charge can come from their core or ligand, and sometimes, the NP coating also plays an important role in defining their charge. Oppositely charged particles are attracted to the surface of NPs, forming a thin layer known as the Stern layer. Since human body cell membranes are negatively charged, positively charged NPs tend to attach themselves to body cells.<sup>112</sup> The penetration of NPs in the human body and their intracellular uptake depend on their surface charge. For this reason, the surface charge of NPs plays a crucial role in their applications in diagnostics and therapeutics. The electric potential at the surface boundary of the double layer ranges from +100 mV to -100 mV.<sup>113</sup> NPs with a zeta potential exceeding +20 mV or falling below -20 mV are resistant to agglomeration and remain stable in solution due to electrostatic repulsion.<sup>114</sup>

### 3.4. Drug loading

The drug loading capacity is an important property in drug delivery systems using NPs. Inefficient drug loading of some nanomedicines poses a hurdle for their practical usage.<sup>115</sup> If drug loading is poor, a greater concentration of

NPs may be required, resulting in a highly viscous liquid that can cause issues for *in vivo* injections.<sup>116,117</sup> Efficient drug loading reduces manufacturing costs.<sup>118</sup> Drug loading capacity is the ratio of the mass of the drug to the total mass of NPs with the loaded drug. Encapsulation efficiency is the ratio of the weight of the drug in the NPs to the weight of the drug added initially during preparation.<sup>119</sup> According to experimental data, drug loading and encapsulation efficiency are highly dependent on the polymer molecular weight,<sup>120,121</sup> drug–polymer interaction, polymer composition,<sup>122</sup> and ending functional groups of the polymer.<sup>123,124</sup>

Three different strategies are employed for drug loading on NPs: (1) pre-loading, (2) co-loading, and (3) post-loading. Fig. 5 provides a visual representation of these three different strategies.

- Pre-loading: drug-loaded NPs are fabricated first, followed by the synthesis of a shell that protects the drug core.<sup>125</sup> The drug loading capacity using this technique is proportional to the shell thickness.<sup>126</sup>

- Co-loading: the drug is loaded into the NPs during their synthesis.<sup>125</sup> Covalent bonding plays a pivotal role along with hydrophobicity,  $\pi$ – $\pi$  interactions, and electrostatic interactions.<sup>127</sup>

- Post-loading: nanocarriers such as carbon and silica are synthesised and mixed with the solution of the drug.<sup>125</sup> The drug is then loaded through various mechanisms such as entrapment, hydrophobic forces, adsorption, and electrostatic interactions.<sup>128</sup>

### 3.5. Drug release

The drug release capacity is a crucial factor in the efficiency of NP-based drug delivery systems. Like poor drug loading, inefficient drug release presents a challenge for the practical implementation of various nanomedicines. The drug release efficiency of NPs is also influenced by the



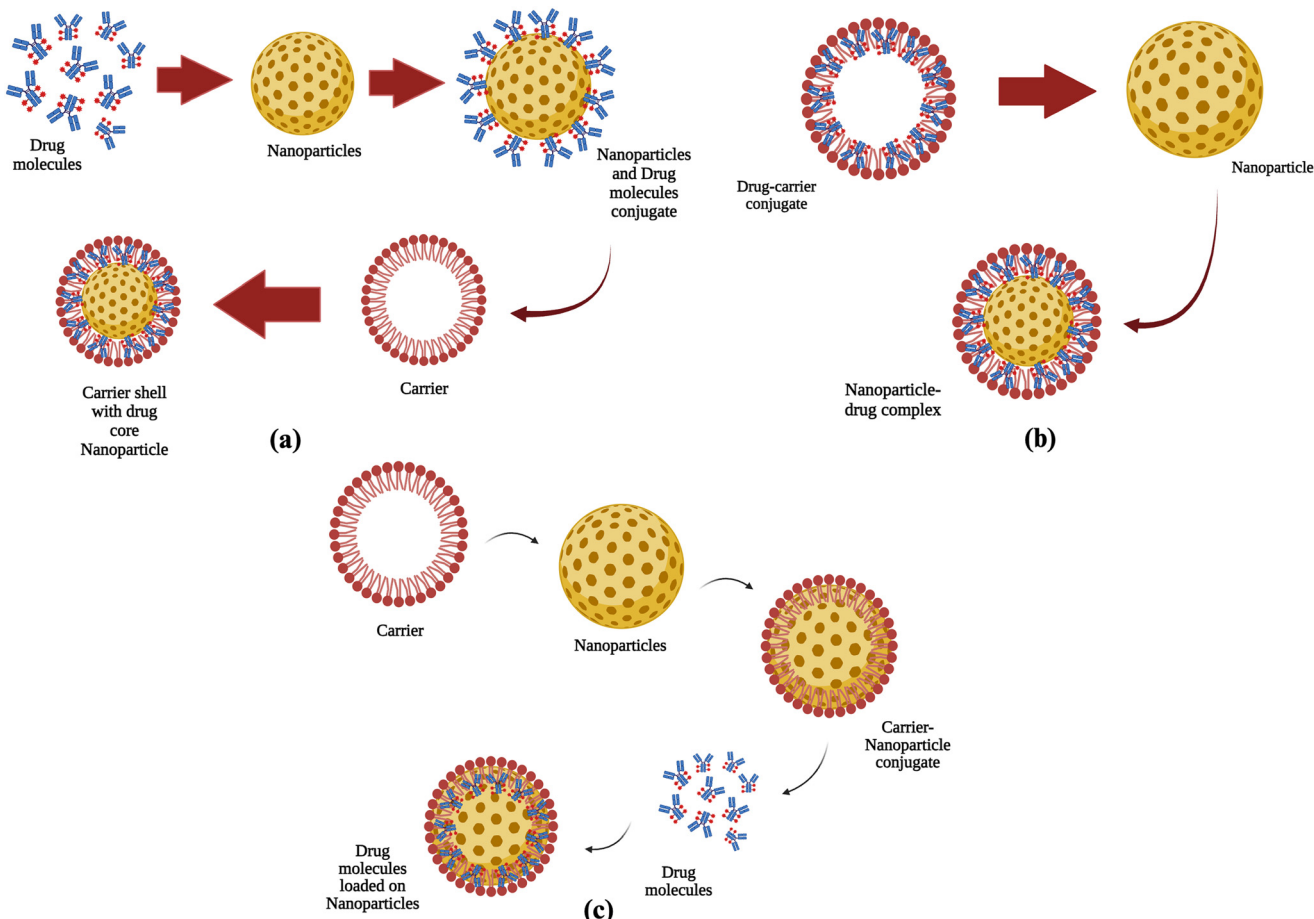


Fig. 5 Schematic illustration of different types of drug loading on the NPs: a) pre-loading, b) co-loading and c) post-loading.

chosen drug loading strategy. For nanosphere-shaped NPs, drug release occurs through matrix erosion,<sup>129</sup> while in the case of nanocapsules, diffusion of the drug through the polymeric layer controls the drug release.<sup>130</sup> Other important factors that generally control the drug delivery are temperature, pH, solubility and desorption of the drug.<sup>131,132</sup>

Auxiliary agents such as polyethylene oxide-propylene oxide (PEO-PPO) can be used to facilitate drug release by weakening the ionic interactions between the drug and NP.<sup>133</sup> Recently, smart NP-based drug delivery systems have been developed. As an emerging area of research, these are capable of releasing drugs in response to particular physiological triggers.<sup>134</sup>

#### 4. Nanoparticle synthesis

There is a wide range of different methods for NP synthesis, and the choice of method depends significantly on the desired properties of the NPs and their intended applications. Two main categories based on the starting point of the procedure are: (1) top-down methods and (2) bottom-up methods. In top-down methods, NPs are synthesised by the breaking down of their bulk constituents, whereas in

bottom-up methods, atoms are clustered into NPs. Table 1 provides a comprehensive overview of the different NP synthesis methods with associated advantages and disadvantages.

Based on the detailed working principles, these methods can also be categorised into: (1) physical, (2) chemical, and (3) biological methods. Physical methods of NP synthesis are typically top-down methods, while biological methods can be considered as bottom-up methods. Chemical methods can follow both bottom-up and top-down approaches. Each method has different advantages and limitations. Recently, researchers have focused on the green synthesis of NPs using non-toxic and environment-friendly reagents. Most biological and chemical synthesis methods are considered green methods, depending on their compatibility with green chemistry principles.<sup>161–163</sup> In this section, we will briefly discuss these methods. Fig. 6 gives a comprehensive overview of different NP synthesis methods. After NP synthesis, different conventional techniques based on an external field (e.g., ultracentrifugation and gel electrophoresis) and sieving (e.g., chromatography and nanofiltration) techniques are employed for NP sorting with desired characteristics.



**Table 1** Comparative analysis of physical, chemical, and biological methods, their benefits, drawbacks, NP synthesis methods, and applications

Category	Advantages	Disadvantages	Synthesis method	Applications
Physical methods	Free of solvent contamination	Abundant waste	Laser ablation	Au, Mg, and Zn NPs synthesized using the pulsed laser ablation in liquid (PLAL) method for antibacterial and biocompatible functionalization of dental implant surfaces <sup>135</sup>
	Uniform monodisperse NPs are synthesized	Less economical		TeO <sub>2</sub> NPs synthesized using the top-ablation and bottom-ablation methods for ultrawide band gap (UWBG) applications <sup>136</sup>
	No chemical purification is required	Potential toxicity		NTO NPs for use as high-performance catalyst supports in polymer electrolyte fuel cells. <sup>137</sup>
	Large scale production	High energy consumption	Spray pyrolysis	ZnO/Ag hollow NPs for enhanced antibacterial activity and visible light-assisted wound healing applications <sup>138</sup>
		Difficult extraction procedure	Magnetron sputtering	W NPs synthesized using magnetron sputtering combined with gas aggregation <sup>139</sup>
				ZrC NPs <sup>140</sup>
Chemical methods	Controllable deposit parameters	Usage of toxic and hazardous chemical reagents		MoC NPs for energy conversion applications. <sup>141</sup>
	Narrower size distribution	Long synthesis time		Ag NPs <sup>142</sup>
	Economical technique	Limitation in increasing batch reactors		Zn NPs <sup>143</sup>
	Production of NPs with thick coating is possible	Chemical purification is required	Sol gel methods	Bimetallic FeCu for multifunctional magnetic-plasmonic applications in biosensing <sup>144</sup>
		Sometimes need to have a large amount of surfactants		Fe doped ZnO NPs <sup>145</sup>
				Niobium-doped titanium dioxide NPs <sup>146</sup>
Biological methods	Biocompatibility and environment-friendly	Low yield		MnO NPs for antimicrobial applications against bacterial and fungal pathogens <sup>147</sup>
	Non-toxic and safe reagents	Long synthesis time		CF NPs for enhanced biomedical performance <sup>148</sup>
	Greater stability of NPs	Limited scalability		Niobium-doped strontium titanate (SrTi <sub>1-x</sub> Nb <sub>x</sub> O <sub>3</sub> , STNO) NPs for enhanced photocatalytic degradation of dyes and antibiotics under UV-A light irradiation <sup>149</sup>
	Diverse nature of NPs		Electrochemical methods	Ag NPs for eco-friendly antibacterial applications in food, cosmetics, and medicine <sup>150</sup>
			Solvothermal synthesis	Ruthenium-doped CF NPs for enhanced nonlinear optical absorption in advanced optical limiting applications <sup>151</sup>
			Microemulsion methods	FeO NPs for advanced material applications. <sup>152</sup>
			Plant extract methods	Au NPs <sup>153</sup>
			Microbial synthesis	FeO NPs <sup>154</sup>
			Algal and fungal-mediated synthesis	Ag NPs <sup>155</sup>
				ZnO NPs <sup>156</sup>
				Ag NPs <sup>157</sup>
				Ag NPs <sup>158</sup>
				Au NPs <sup>159</sup>
				ZnO NPs <sup>160</sup>

#### 4.1. Physical methods

Physical methods employ different kinds of physical processes to apply high-energy radiation to different types of energy, such as thermal energy, electrical energy and mechanical pressure on the material. It results in condensation, abrasion, evaporation or melting of the substrate material, which leads towards the synthesis of NPs. These methods are categorised based on the physical process used and their impact on the substrate material. Laser ablation, spray pyrolysis, magnetron sputtering, ion implantation, inert gas condensation, and high-energy ball milling are very commonly used physical methods for NP synthesis.

In the laser ablation method, a laser beam is focused on the target material, causing laser-induced vaporisation and condensation, which leads to the synthesis of NPs.<sup>164,165</sup> Gold (Au), magnesium (Mg), and zinc (Zn) NPs have been

synthesized using pulsed laser ablation in liquid (PLAL) for antibacterial and biocompatible functionalization of dental implant surfaces.<sup>135</sup> Mercury iodide (HgI<sub>2</sub>) NPs have been synthesised with size 25–75 nm using laser ablation.<sup>166</sup> Tellurium dioxide (TeO<sub>2</sub>) NPs have been synthesized using the top-ablation and bottom-ablation methods for ultrawide band gap (UWBG) applications.<sup>136</sup> The spray pyrolysis method involves spraying a precursor material solution using a nano-porous atomiser on the hot substrate of the material.<sup>167</sup> This method has been employed to generate iron-doped TiO<sub>2</sub> NPs with an average size of 12 nm.<sup>168</sup> Carbon-based NPs with an average size of 60 nm have also been prepared by spray pyrolysis.<sup>169</sup> Niobium-doped tin oxide (NTO) NPs were synthesized using spray flame synthesis for use as high-performance catalyst supports in polymer electrolyte fuel cells.<sup>137</sup> ZnO/Ag hollow NPs were synthesized using a one-step spray pyrolysis method for enhanced antibacterial activity and visible light-assisted wound healing



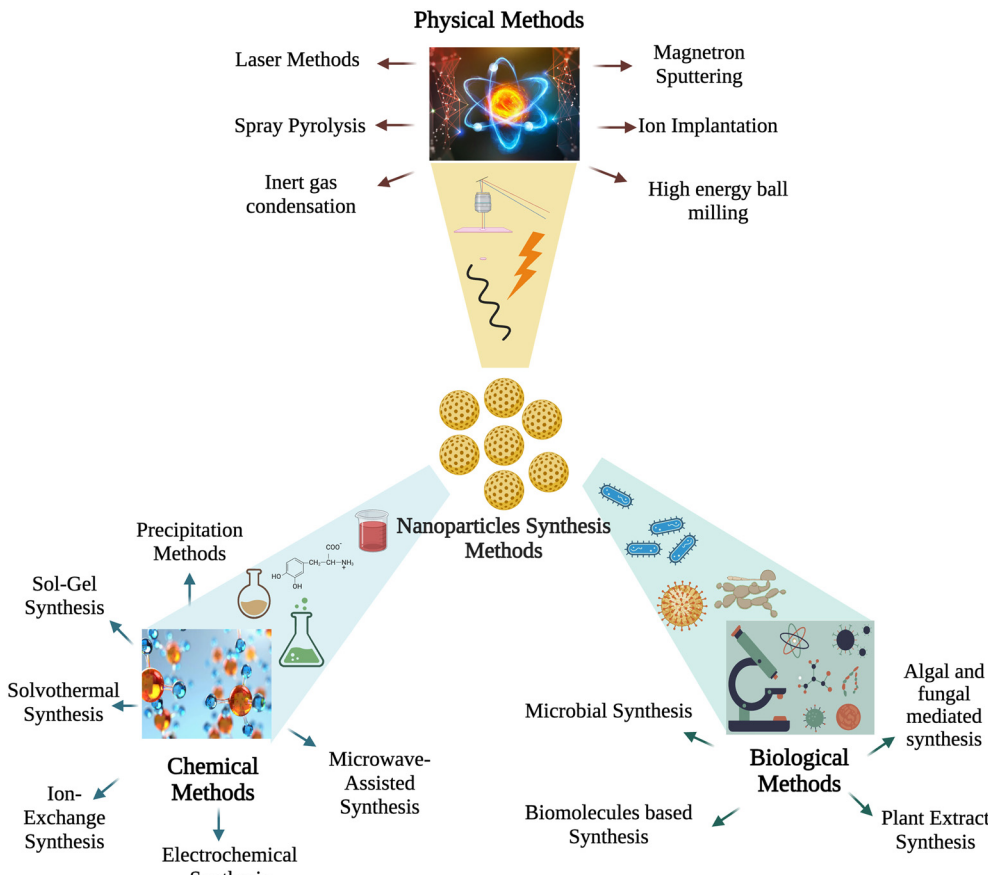


Fig. 6 Comprehensive overview of physical, chemical, and biological methods for NP synthesis.

applications.<sup>138</sup> Magnetron sputtering involves subjecting a target material to high-energy ions, resulting in the ejection of atoms from the targeted material, and the deposition of these atoms leads to the synthesis of NPs.<sup>170</sup> Tungsten NPs (W NPs) and Cu NPs with average sizes of 70 nm and 60 nm have also been synthesized using this method.<sup>171,172</sup> Zirconium nitride (ZrN) NPs were synthesized using reactive direct current magnetron sputtering in an argon and nitrogen atmosphere for environmentally friendly, annealing-free production of plasmonic nanofluids with enhanced optoelectronic properties.<sup>140</sup> The ion implantation method is based on principles of ion–solid interactions, where high-energy ions are bombarded on the substrate material for NP synthesis.<sup>173</sup> Ag NPs and plasmonic-based NPs have been synthesized using this method.<sup>174,175</sup> Molybdenum carbide (MoC) NPs were synthesized using ion implantation at room temperature for energy conversion applications.<sup>141</sup> In the inert gas condensation method, evaporated materials are transported with inert gases, such as He, Ne, Ar, etc. Liquid nitrogen is used as a cooling medium for condensation.<sup>176</sup> Highly size-controlled NPs can be synthesized using this method with particle sizes ranging from 1–5 nm.<sup>177</sup> Bimetallic FeCu NPs were synthesized using the inert gas condensation technique for multifunctional magnetic–plasmonic applications in

biosensing.<sup>144</sup> NP fabrication using high-energy ball milling introduces kinetic energy from the moving balls to break the chemical bonds of the substrate material being milled.<sup>178</sup> Otis and Chin fabricated ZnO NPs and iron sulphide-based NPs (e.g., FeS and FeS<sub>2</sub> NPs) using high-energy ball milling.<sup>179,180</sup>

#### 4.2. Chemical methods

Chemical methods for NP synthesis are based on the chemical reaction between different chemical reagents under various chemical and physical conditions that control the physical and chemical properties of NPs. Precipitation methods, sol–gel methods, electrochemical methods, solvothermal synthesis methods, and microemulsion methods are some of the most commonly used and practically feasible chemical methods for NP synthesis. Manganese oxide (MnO) NPs were synthesized using a simple and cost-effective co-precipitation method for antimicrobial applications against bacterial and fungal pathogens.<sup>147</sup> Cobalt ferrite (CF) NPs were synthesized using this method with polyvinyl alcohol modulation for tunable morphology, magnetic behavior, and enhanced biomedical performance.<sup>148</sup> Niobium-doped strontium titanate (SrTi<sub>1-x</sub>Nb<sub>x</sub>O<sub>3</sub>, STNO) NPs were synthesized using

a microwave-assisted sol-gel auto-combustion method for enhanced photocatalytic degradation of dyes and antibiotics under UV-A light irradiation.<sup>149</sup>

Electrochemical methods use the electrochemical reaction for NP synthesis. An electric current is passed between the anode and cathode, which are immersed in the electrolyte, a solution of precursor material ions.<sup>181</sup> ZnO NPs with a diameter range of 50–100 nm were synthesised using this method.<sup>182</sup> Ag NPs were also synthesized using an electrochemical method with *Camellia chrysanthia* flower extract as a green electrolyte, reducing agent, and stabilizer for eco-friendly antibacterial applications in food, cosmetics, and medicine.<sup>150</sup> Solvothermal synthesis involves boiling the precursor material in a closed reaction system that creates a high-pressure environment, leading to NP synthesis.<sup>183</sup> Iron-doped tin sulphide NPs (SnS NPs) with supercapacitive and magnetic properties have also been used.<sup>184</sup> Ruthenium-doped cobalt ferrite NPs were synthesized using a modified solvothermal method for tunable magnetic behaviour and enhanced nonlinear optical absorption in advanced optical limiting applications.<sup>151</sup> Microemulsion techniques use the concepts of interfacial chemistry, colloidal science, and thermodynamics for NP synthesis. This system consists of monodispersed spherical droplets of two immiscible liquids, depending on the surfactant.<sup>185</sup> Size-controlled Ag NPs have been made by using water in an oil microemulsion.<sup>186</sup> Iron oxide (FeO) NPs were synthesized using a microemulsion-hydrothermal method for controlled production of nanorods and nanospheres with tunable size, shape, and magnetic phase for advanced material applications.<sup>152</sup>

#### 4.3. Biological methods

Biological methods for NP synthesis are the result of a synergistic interaction between nanotechnology and nanobiotechnology. These methods utilise extracts from living organisms—such as algae, fungi, plant extracts, bacteria, viruses, and yeast—or biomolecules like enzymes to synthesise NPs. Biological methods are considered to be green synthesis because they are non-toxic and environmentally friendly. Biological methods can be categorised into four sub-categories depending upon the biological system being used for NP synthesis: (1) plant extract methods, (2) enzyme-based synthesis, (3) microbial synthesis, and (4) algal and fungal mediated synthesis.

Plant extract-based methods use plant biomass or plant extract as reducing, stabilizing, and capping agents, leading towards the synthesis of a wide array of inorganic NPs including Au, Ag, TiO<sub>2</sub>, ZnO, Fe, Cu, Se, and Pd.<sup>187</sup> These reducing agents convert metal ions into metal NPs. Among the most promising green-synthesized nanoparticles are FeO NPs which have gained traction for their role in cancer diagnosis and treatment. Importantly, the utilization of waste plant materials makes this type of NP synthesis eco-friendly

by addressing concerns related to resource efficiency and environmental impact.<sup>154</sup>

Biomolecule-based NP synthesis uses various biomolecules, such as nucleic acids, viruses, enzymes and membranes. Biominerallisation<sup>188</sup> and biomimicry<sup>189</sup> are the foundation phenomena for such synthesis techniques. Microbial-based synthesis employs different types of microorganisms, such as bacteria, yeast and actinomycetes, as bioreactors for NP formation. These microorganisms convert the metal ions to element metal through their cellular activities.<sup>190</sup> Algal-mediated NP synthesis uses algae's ability to hyper-accumulate heavy metal ions and their extraordinary capability to transform these metal ions into more malleable forms.<sup>191</sup> Fungal-mediated NP synthesis uses various biomolecules produced by fungi, such as enzymes, polysaccharides, and proteins, as reducing agents, stabilisers and templates for NP synthesis.<sup>192</sup>

#### 4.4. Nanoparticle sorting techniques

While the synthesis is concerned with the fabrication of NPs, sorting is an essential subsequent step to ensure the homogeneity and consistency of NPs, especially for their practical applications. To create batches of NPs with uniform properties after their synthesis, different sorting techniques are applied, which separate NPs based on various physical properties, *e.g.*, size, shape and surface charge. Several conventional methods have been employed for NP sorting that range from physical methods, *e.g.*, centrifugation and electrophoresis, to sieving techniques, *e.g.*, chromatography and nanofiltration. Table 2 provides a comparative overview of the different NP sorting techniques.

**4.4.1. Ultracentrifugation.** Ultracentrifugation separates NPs based on the external centrifugal force created by the rotation of the centrifuge, with separation based on size and shape.<sup>202</sup> NPs dispersed in a mixture of miscible organic solvents are separated based on different sedimentation rates. Ultracentrifugation techniques can be divided into two most widely used subtypes: (1) analytical ultracentrifugation sedimentation velocity (AUC-SV) and analytical ultracentrifugation sedimentation equilibrium (AUC-SE).

In AUC-SV, complete sedimentation of the sample is achieved using a strong centrifugal field, while AUC-SE is performed in a comparatively low centrifugal field. Although both AUC-SV and AUC-SE are applicable to sort NPs into concentration gradients, AUC-SE has the advantage of inhibiting any transport as the concentration gradient stays constant in the equilibrium state.<sup>203–205</sup> Sorting of Au nanorods has been performed by employing multiwavelength analytical ultracentrifugation.<sup>206</sup> Optimal precursor concentrations identified by AUC have been used to get well-dispersed polystyren@ZIF-8 core–shell NPs.<sup>207</sup> Recently, ultracentrifugation has also been successfully employed for density-based separation of mRNA-loaded lipid nanoparticles (LNPs), enabling resolution into subpopulations with distinct

**Table 2** Comparative overview of different physical and sieving sorting methods, working principles, their advantages and disadvantages

Technique	Working principle	Advantages	Disadvantages	NP sorted
Ultracentrifugation	Centrifugal force generated by rotation	Formation of concentration gradient	Sample loss	Analytical ultracentrifugation technique for polystyrene-ZIF-8 core-shell NPs <sup>193</sup>
	NPs are separated on the basis of size and shape.	Excellent results for ordering NPs as richer structures Stable and biocompatible NP synthesis	Chances for aggregation are always high	Density-based separation of mRNA-loaded lipid NPs (LNPs) <sup>194</sup>
Gel electrophoresis	External electric field through a porous gel	Multiple runs in parallel	Expensive and unapplicable for commercial use due to the requirement for specialized equipment NP morphology becomes tedious due to irreversible agglomeration or accumulation	Slab gel electrophoresis technique for TiO <sub>2</sub> NPs <sup>195</sup>
	NP separation based on size, shape, charge and exact number of attached polymer chains		Batch-limited technique due to the requirement of multiple steps Long time required for sample separation	DNA-assisted electrophoresis technique for NPs <sup>196</sup>
Chromatography	Sieving technique	High separation efficiency	Sample retrieval is very complicated Long time requirement	Bed chromatography technique for sorting of magnetic NPs <sup>197</sup>
	NPs are separated in a mobile phase through a stationary phase	Very few chances for NP agglomeration and accumulation	Multiple sample preparation	Size exclusion chromatography for metal-based NPs <sup>198</sup>
	NPs are separated on the basis of size, shape and surface properties	No sample loss	Specialised beads, antibodies and buffers for separation	Optical chromatography technique using 3D-printed microfluidic devices for particle separation <sup>199</sup>
Nanofiltration	Sieving technique based on membrane filtration	Less expensive technique Fast, small amount of solvent required, and can be scaled up for commercialisation	Clogging of nanofiltration membrane	Graphene oxide nanofiltration membrane for Ag NPs <sup>200</sup>
	NPs are separated on the basis of size and shape		Physiochemical reactions between membrane and NPs NP morphology becomes tedious	Supramolecular membrane for NP separation based on size <sup>201</sup>

biophysical and functional properties, including differences in *in vivo* protein expression.<sup>194</sup>

Despite its widespread use for NP sorting, ultracentrifugation has several limitations that make it less efficient. Separation is based on a density gradient, and achieving a prerequisite density gradient is necessary to achieve higher-quality separation at the nanoscale. Additionally, sample loss is inevitable during the purification process, as large gravity force exposure to particles can result in aggregation. Furthermore, specialised equipment requirements make it impractical for large-scale industry use.<sup>208,209</sup>

**4.4.2. Gel electrophoresis.** Gel electrophoresis (Gel-EP) is a technique that uses electric fields to sort NPs. The NPs are propelled by a voltage gradient through a gel that contains small pores. Gel-EP sorts the NPs according to size, shape, charge, and the number of polymer chains attached.<sup>210–212</sup>

Gel-EP and pH control have been used to differentiate and separate nanospheres with identical sizes but varying anionic surface charges.<sup>213</sup> Recent advancements have highlighted the use of DNA as a programmable and biocompatible tool to assist NP separation by modulating their physical properties—such as size, charge, and mass enhancing Gel-EP's specificity and control.<sup>196</sup> Moreover, genome-wide genetic screening has revealed that NPs interact with multiple cellular receptors, such as LDLR, SCARB1, and heparan sulfate, offering new insights into NP behavior and potential adaptations for separation strategies.<sup>214</sup>

Gel-EP allows parallel runs on the same gel, providing a significant advantage over other conventional techniques for NP synthesis, such as ultracentrifugation, chromatography, and nanofiltration. This advantage is particularly important for mechanism understanding and optimising conditions.<sup>215</sup> Recently, Gel-EP has been used to purify photon-



upconversion NPs for large-scale analogue and digital bioassays.<sup>216</sup> However, this technique is batch-limited and requires multiple steps, making it time-consuming and challenging for sample retrieval.<sup>217</sup>

**4.4.3. Sieving techniques.** In sieving techniques, physical holes or barriers in the form of membranes or columns are used for NP separation. The two most commonly used sieving techniques are (1) chromatography and (2) nanofiltration.

*Chromatography.* This technique achieves sample separation through a stationary phase suspended in a mobile solvent phase. The rate of separation is determined by the particle's partitioning speed through the stationary phase. There are several different types of chromatography for NP synthesis, such as ion-exchange chromatography, size-exclusion chromatography, high-performance liquid chromatography, and affinity chromatography.

A novel magnetic chromatography method has been employed for efficient and large-scale sorting of magnetic NPs.<sup>218</sup> Pitkanen provided an extensive review of size-exclusion chromatographic separation and characterisation of noble metal-based NPs and quantum dots.<sup>219</sup>

Incorporating recent advances in lab on a chip technologies, 3D-printed microfluidic devices have been used to perform optical chromatography for the separation of micron-sized particles based on size and refractive index. These devices, integrated with single-mode optical fibers and designed with hydrodynamic focusing features, demonstrate efficient optofluidic trapping and sorting capabilities, pointing to a promising future for combining chromatography with additive microfluidic platforms.<sup>199</sup> This technique can deliver high separation efficiency, but it is time-consuming and requires multiple preparation steps. Additionally, separation requires specialised beads and buffers.<sup>220</sup>

*Nanofiltration.* This sieving technique for NP synthesis uses a filtration membrane, and different membrane materials have been synthesised and used for nanofiltration. NPs that are smaller than a particular cut-off size of the nanofilter's pores are allowed to pass through. Yang examined the impact of silver NP size on the nanofiltration performance of graphene oxide/sAG composite membranes, finding the optimal NP size for water flux and dye rejection.<sup>221</sup> A robust, reusable nanostructured supramolecular membrane has been developed by Krieg, which is capable of size-selective separation of metal and semiconductor-based NPs, utilising the strength of hydrophobic interactions and the reversible nature of noncovalent bonds for easy disassembly, cleaning, and reassembly.<sup>222</sup>

Recent advancements in membrane design further enhance this technique's performance. A study demonstrated the development of a polyethersulfone-based nanofiltration membrane functionalised with green-synthesised copper phosphide ( $\text{Cu}_x\text{P}$ ) NPs, which achieved a 98.72% pesticide rejection rate and significantly improved water flux and antifouling properties, showcasing potential for agricultural

waste water treatment.<sup>223</sup> Additionally, incorporation of calcium carbonate ( $\text{CaCO}_3$ ) NPs into thin-film nanocomposite membranes has proven to overcome the traditional trade-off between permeability and selectivity. The resulting membranes demonstrated 1.7-fold higher permeability compared to conventional TFC membranes while maintaining high salt rejection.<sup>224</sup>

Nanofiltration is considered a fast technique for NP sorting and requires minimal solvent volume. It can be scaled for industrial applications to sort large samples. However, filtration membranes can become easily clogged, leading to particle aggregation and decreased sorting efficiency. Multiple steps are required to sort samples with different particle sizes.

Observing the data presented in Tables 1 and 2 which depicts different NP synthesis and sorting methods, and in light of the critical performance parameters of NPs for drug delivery systems outlined in section 2, it becomes clear that addressing the shortcomings of traditional NP synthesis and sorting techniques is of paramount importance. The concept of an optimal NP synthesis method would ideally allow for facile control of output properties such as size, shape, and surface characteristics while maintaining a minimal usage of reagents. Such a method would not only be economically efficient but also environmentally friendly. Microfluidics is a notable technique for making NPs with particular attributes. It offers a better way of creating and sorting NPs compared to other traditional techniques. The following section provides a comprehensive explanation of NP creation based on microfluidics.

## 5. Microfluidics

Microfluidics involves the design and fabrication of devices with various geometries of chambers and microchannels for precise control, processing, or manipulation of very small volumes of fluids ( $10^{-9}$  to  $10^{-18}$  L).<sup>225,226</sup> It can reduce and eliminate many of the limitations of conventional techniques, such as sample loss, long duration, and large volume requirement, and can offer better control on NP characteristics, *e.g.*, size, morphology and surface properties, as well as better separation resolution.<sup>208</sup> It falls into the chemical synthesis category as it mostly uses the nanoprecipitation principle that dissolved in water-miscible solvents, hydrophobic solutes precipitate when mixed with antisolvents.<sup>26,27,227,228</sup> Fig. 7 depicts a simple illustration of the microfluidic-based NP synthesis. Different reacting reagents are manipulated in microchannels that lead towards their mixing in a controlled way, which results in the synthesis of NPs. Different types of flow systems can be involved in the microfluidic chip for NP synthesis *i.e.* single phase flow system, gas liquid flow system, and liquid–liquid flow system.<sup>26</sup> Table 3 provides a brief overview of the benefits and drawbacks of NP synthesis using microfluidic-based technology.

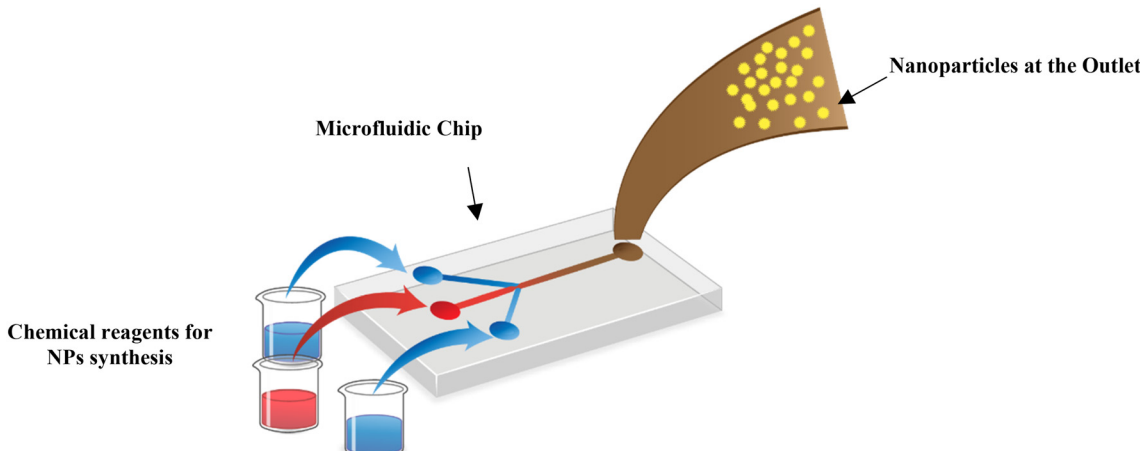


Fig. 7 Schematic diagram of NP synthesis in a microfluidic channel.

Table 3 Advantages and disadvantages of microfluidic devices

Advantages	Limitations
<p>Very highly reproducible synthesis technique<sup>229</sup></p> <p>Reagent consumption is lower than in other techniques</p> <p>Easy to control experimental parameters <i>e.g.</i> flow rate, pH, temperature, and concentration of reagents<sup>233,234</sup></p> <p>Less time consumption</p> <p>Easy to commercialise the production<sup>235</sup></p>	<p>Sometimes fouling and channel clogging<sup>230</sup></p> <p>Diffusion of NPs in PDMS matrix<sup>231</sup></p> <p>Not fully automated chip formation<sup>232</sup></p>

In a microfluidic system, different factors, such as fluidic resistivity, fluidic diffusivity, and viscosity, play important roles in performance rather than just dominant inertial force, as in the case of typical macrofluidic-based flow systems.<sup>236,237</sup> Due to the relatively low velocity combined with the small-scale hydraulic diameter, a low Reynolds number (Re) causes intrinsic laminar flow within the microfluidic channels. Molecular diffusion and advection are two different phenomena responsible for the mass transfer. In molecular diffusion, molecules migrate across the fluidic interface, while in advection, mass is directly carried by fluid flow.<sup>238</sup> Usually, molecular diffusion is the main mechanism for mixing, as laminar flows make mixing particularly difficult due to convective mass transfer in the flow direction.<sup>239</sup> Mixing is promoted by using different methods, typically by manipulating the flow-through channel geometry or external disturbances.<sup>240</sup> According to these methods, microfluidic-based technology is divided into two categories: (1) passive methods without external sources and (2) active methods requiring external sources. The mixing process is considered to be the most critical step for producing NPs with desired physical and chemical characteristics.<sup>241</sup> Microfluidic systems have been increasingly investigated as methods to efficiently tune mixing. With exact control of parameters such as fluid concentration ratio, flow rates, and temperature, the ability to rapidly mix fluids in a homogeneous environment can be

improved, resulting in improved product quality.<sup>242,243</sup> Well-controlled tunability of the nucleation rate, homogeneity and physicochemical characteristics of NPs can be achieved by systematically screening the parameters used for micromixing in microfluidic devices.<sup>244,245</sup>

As this precise control of NP properties requires a continuous repetition of experiments to tune the flow parameters accordingly, which leads to the waste of time and resources, currently, microfluidic systems are being integrated with artificial intelligence.<sup>246</sup> Deep learning and machine learning algorithms, artificial neural networks (ANN), and advanced graphics processing units (GPU) have led to very rapid structured data analysis to predict accurate complex outputs.<sup>247</sup> Combining microfluidic chips with data-acquisition instrumentation, along with multimodal monitoring, can lead to advances in the field of online sensing of NP properties.<sup>246,248</sup>

### 5.1. Passive microfluidics

Passive microfluidic (PM) chips operate on the principle that embedded micromixers function without any external sources to aid the mixing process.<sup>249</sup>

This type of chip is particularly suitable for fabricating NPs that are sensitive to external factors, such as thermal, acoustic, and electromagnetic conditions. Various geometries and techniques are employed to enhance the mixing of initial



Table 4 NPs synthesis by different passive microfluidic techniques

Passive microfluidic method	NP synthesised
Hydrodynamic flow focusing	PEG-PLGA NPs for controlled drug delivery synthesized using a sudden expansion microreactor <sup>250</sup> Liposomal NPs for cancer therapy <sup>251</sup> Hybrid NPs for enhancing blood flow and heat transport in stenosed arteries <sup>252</sup>
Micro vortices	Salicylic acid-functionalized $\text{Fe}_3\text{O}_4$ core-shell NPs for applications in biomedicine and environmental remediation <sup>253</sup>
Chaotic advection	$\text{ZnO}$ NPs using spiral microfluidic reactor <sup>254</sup> $\text{CuO}$ NPs for enhanced antimicrobial and antioxidant activities <sup>255</sup> Cationic and stealth liposomes for high-throughput nanomedicine production synthesized using a 3D multihelical chaotic-advection microfluidic device <sup>256</sup>
Droplet-based methods	Calcium peroxide (CP)-based oxygen-releasing microgels for tissue engineering applications <sup>257</sup> Synthetic cells such as liposomes, polymersomes, and coacervate microdroplets for biomimetic and biomedical applications <sup>258</sup> Cell-encapsulating microcarriers for tissue engineering and regenerative medicine <sup>259</sup>

fluids in passive microfluidics, making it a cost-effective and efficient alternative to active microfluidic chips.

Four main methods are commonly used to enhance mixing in passive microfluidic systems: hydrodynamic flow focusing, vortex methods, chaotic advection, and droplet-based methods. Table 4 provides examples of NP synthesis using these different passive approaches.

**5.1.1. Hydrodynamic flow focusing.** In hydrodynamic flow focusing (HFF), a core fluid in the centre of the channel is sheathed by the fluid flowing along the sides to convert it into a narrow stream (Fig. 8). There is always a very high flow rate ratio (FRR), typically greater than 10, between the sheath flow and central flow. A higher surface-to-volume ratio at the core–sheath fluid interface and a higher concentration gradient can be achieved with an increase in FRR. It also leads to the compression of the core fluid flow due to the low flow rate, which becomes responsible for a significant reduction in the time required for mixing because of the reduction of the required diffusion length. This improves the quality and homogeneity of NPs, especially when they are being synthesised by a bottom-up approach like nanoprecipitation.<sup>260</sup> Isolation of the precipitation in microchannel walls is a challenge for efficient mixing in 2D flow focusing. 3D HFF provides a solution to this problem whereby the central flow provides horizontal and vertical flow focusing.

**5.1.1.1. Coaxial tube micromixers.** Two concentric capillary tubes are used in this type of micromixer, which is connected at the central flow terminal. The inner capillary tube controls the central flow, while the outer tube facilitates the sheathed or side flow (Fig. 8c). The central flow size and pattern can be controlled by different parameters, such as tube geometry, fluid physical properties and FRR.<sup>260</sup> As the FRR is directly proportional to the flow rate of the sheath flow, the flow in the central layer becomes narrower and narrower, leading to the formation of jetting flow. High-throughput coaxial tube micromixers have been used for siRNA-polyelectrolyte polyplex NP synthesis.<sup>262</sup> Au and Ag NPs have also been synthesized by hydrodynamic flow focusing in coaxial tubes. The properties

of these NPs can be tuned by controlling the mixing by varying the diameters of co-axial tubes.<sup>263</sup>

**5.1.1.2. Chip-based hydrodynamic flow focusing.** Chip-based flow synthesis is a cost-effective method due to its ease of mass manufacturability. Chip reactors are primarily fabricated using different techniques, such as soft-lithography and replica modelling. Integrating additional on-chip functions, including electrochemical and optical sensors, as well as microheaters, is also possible.<sup>264</sup> 2D HFF in microfluidic systems is achieved through a horizontally focused central flow.<sup>265</sup> The most straightforward design involves a core flow sheathed by two side fluid streams.<sup>266</sup> Using this geometry, mixing can be made highly efficient, with a mixing time of less than 50  $\mu\text{s}$ . The sheath-flow channel can have different orientations and be tilted to a different inlet angle other than 90° to ensure stability in the flow profile. 3D HFF can further improve the size uniformity of the NPs by applying both horizontal and vertical focusing at the same time (Fig. 8d). Different techniques are used to make the 3D HFF system more economical by reducing the number of layers. This method is highly effective, fast, and economical as it does not require complex fabrication techniques other than soft lithography.<sup>267,268</sup>

Using 3D HFF, PLGA-PEG NPs with a size range of 50–150 nm have been successfully synthesised. HFF-based microfluidic systems are capable of providing a robust production rate for NP synthesis up to 288 mg  $\text{h}^{-1}$  using a single device, compared to conventional microfluidic devices without HFF.<sup>269</sup> Doxorubicin (DOX/PCL) NPs with a uniform size range of 120–320 nm with high drug encapsulation efficiency between 48% and 87% have been achieved using an HFF microfluidic device. Additionally, the production process can result in highly stable encapsulation efficiency of the DOX drug, as the release profile of DOX/PCL NPs was sustained for 10 days at pH 7.4.<sup>270</sup>

**5.1.2. Vortices.** Microvortices address the inefficiency of slow diffusive mixing and the generation of undesirable waste, such as polymer aggregates. Specific microstructures



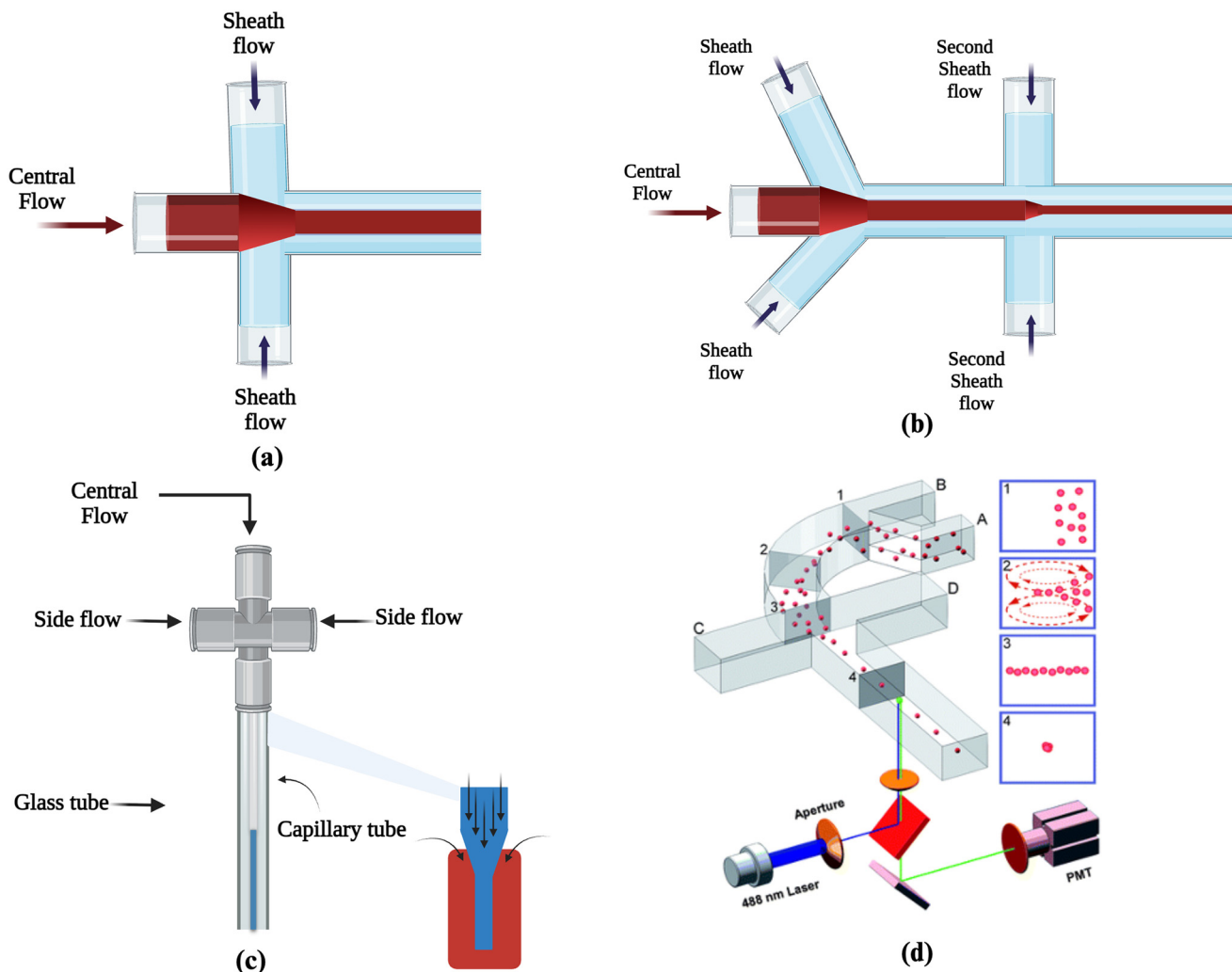
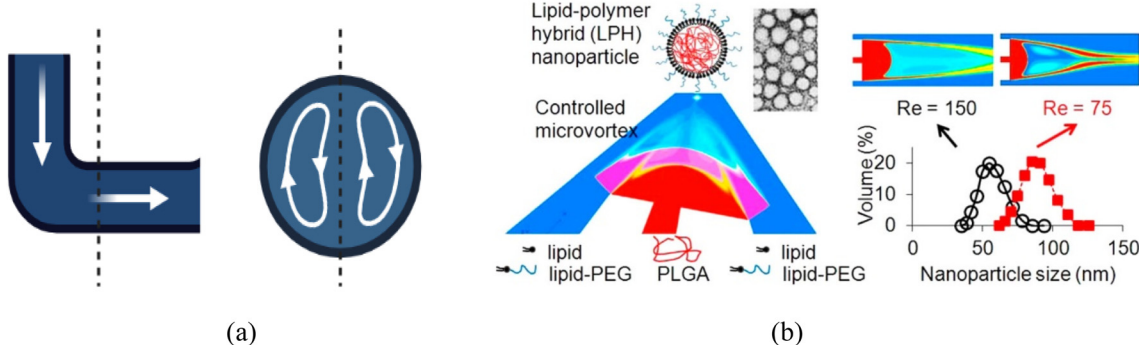


Fig. 8 Schematic diagrams of a) single and b) double lamination-based HFF; c) schematic diagram of coaxial tube-based HFF; d) schematic diagram of 3D flow focusing, A: particles; B: sheath flow for vertical flow focusing; C and D: sheath flows for horizontal focusing adapted from<sup>261</sup> Copyright (2009) Royal Society of Chemistry.

and microchannel geometries lead to the formation of mixing-enhancing vortices. These microvortices can be 2D or 3D and have practical applications in NP synthesis with desired characteristics. Anisotropic flow resistance can be induced by placing ridges in microchannels with an oblique angle. This anisotropic flow resistance generates secondary flow across the cross-section of the microchannel (Fig. 9a). To increase the surface-to-volume ratio and concentration gradient, ridges are normally arranged in a herringbone pattern. Based on theoretical and experimental data, it can be concluded that the mixing length is far less in cases of 2D vortices compared to diffusive mixing length without a vortex.<sup>271</sup> Microvortices form at the curved or sudden expansion of microchannels due to mismatching velocity in different portions of the fluid when the Re number exceeds 1. The Re number, a dimensionless quantity in fluid mechanics, represents the ratio of inertial forces to viscous forces within a fluid flow. This indicates

that fluid inertia is more significant than viscous forces when  $Re > 1$ . As the Re number increases, indicating a greater dominance of inertia over viscosity, the vortices become more intense.<sup>272</sup>

Another inertia-based mixing strategy is the introduction of secondary flow along the curved microchannels. A Dean vortex is generated due to the difference in inertia because of the parabolic velocity profile, which leads towards fast central flow and slow side flow. Dean vortices typically manifest as a pair of oppositely rotating vortices, which direct outwards at the centre of the microchannel while inwards near the bottom and top walls. Due to the intrinsic helical chirality in 3D vortices, self-assembly of molecules and hydrodynamic chiral effects are also exerted.<sup>274</sup> The difference in flow velocities between the microchamber and the main channel creates laminar vortices (counterclockwise/clockwise) in the opposite microchamber.<sup>275</sup> Microvortices



**Fig. 9** a) Schematic diagram of secondary flow in a microchannel; b) schematic cross-sectional view of a three-inlet microfluidic system used for the synthesis of lipid-polymer hybrid NPs with the help of microvortices adapted with permission from<sup>273</sup> Copyright (2012) American Chemical Society.

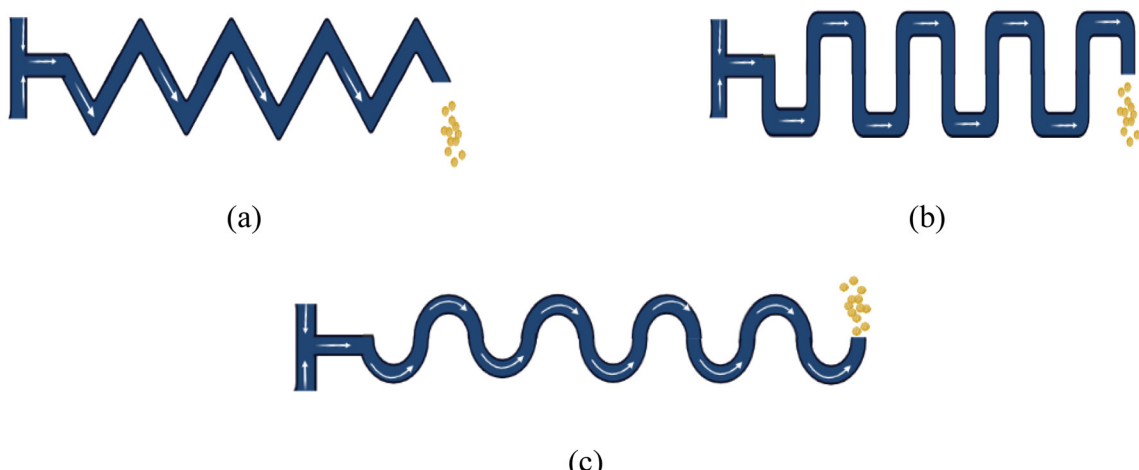


**Fig. 10** Schematic diagram of different shaped microchannels for better mixing a) zig-zag b) square c) serpentine shaped microchannels.

can deliver productivity 1000 higher compared to simple diffusion-based mixing in the case of lipid-polymer NP synthesis. An efficient microfluidic platform for NP synthesis based on microvortices was proposed. It was suggested that the NP size can be controlled by regulating the mixing through microvortices (Fig. 9b).<sup>273</sup> 3D microvortex-based microfluidic platforms have been employed for the synthesis of homogenous PLGA NPs with tunable properties.<sup>276</sup>

**5.1.3. Chaotic advection.** Stretching and folding of fluid that leads towards chaotic advection can also be used in the microchannels to enhance mixing.<sup>277</sup> Different kinds of geometries, *e.g.* spiral, zigzag and serpentine, can be used to create chaotic advection that leads towards the synthesis of NPs.<sup>278–280</sup> Fig. 10 shows zig zag, square and serpentine-shaped channels that can lead towards better mixing. Chaotic advection can also be achieved by modifying the microchannel walls with obstacles to disrupt the flow. Mixing, in the case of staggered obstructions, is 5% higher than symmetric

obstructions due to the cross-stream velocity component. The efficiency of mixing is directly proportional to the number of obstructions because of the increased residence time in the region of obstruction. Obstructions with large widths and depths can lead to a large turn of the flow, generating higher secondary flow and leading to a higher mixing efficiency. Radial baffles can also be introduced in the curved-shaped microchannels to enhance mixing. Baffled-based microfluidic chips have been developed for the synthesis of silica NPs.<sup>281,282</sup> The chaotic advection principle can be combined with a split-and-recombine principle for enhanced mixing. Efficient mixing can be achieved over a large range of  $Re$  numbers with the help of 3D convoluted channels.<sup>283</sup> Combining a zig-zag channel path with a split-and-recombine arrangement can lead to multiple mixing mechanisms, including twisting, splitting, recombining, vortices and transversal flows, and chaotic advection. This type of arrangement can deliver 90% mixing efficiency with a flow of  $20 \leq Re \leq 0.9$ .<sup>284</sup>



Modifications in the microchannel wall are a very well-established technique for chaotic advection creation when the flow is laminar with a low  $Re$  number. Incorporating slanted grooves and staggered herringbone grooves is commonly used for modifying a microchannel wall, which leads to transversal secondary flow. The stretching of fluidic elements occurs in a transverse direction due to the inclined orientation of the grooves about the channels. This increase in fluid interface enhances mixing through diffusion. Herringbone pattern-shaped microfluidic devices also provide a very controllable and reproducible NP synthesis platform. 3D printing of herringbone patterns is also proposed for lipid–polymer hybrid NP synthesis.<sup>285</sup>

**5.1.4. Droplet-based methods.** These methods are highly efficient and require low volume for screening and analysis.<sup>286</sup> Multiple droplets are generated, which act as individual reaction units. Droplet-based methods can work under extreme conditions at high temperatures and in the presence of aggressive reagents. Highly reproducible and homogenous NPs with controllable size can be synthesised using this method.<sup>287</sup> It is considered the most robust fabrication method as it can synthesise drug carriers with advanced features, such as multifunctionality and size tunability. Multiple-step synthesis of NPs with a millisecond timescale can also be performed using the droplet-based microfluidics method.<sup>288</sup> Three different kinds of microfluidic structures are used to generate droplets: (1)

cross-flowing, (2) co-flowing, and (3) flow-focusing. Fig. 11 provides a schematic depiction of these three different methods.

1. Cross-flowing is based on a T-junction with two channels intersecting at a crossing angle of  $90^\circ$ . From the side of the microchannel, a discrete phase is introduced into an already running continuous phase. There can be different orientations for the introduction of side flow, leading to increased shear stress and accumulated pressure, converting the discrete phase into droplets. Research has been done on the dynamic behaviours of droplet formation in microfluidic cross-junction devices using a two-dimensional numerical model. It has been reported that the junction angle and viscosity ratio significantly influence the droplet size and frequency of generation, and these insights could be pivotal for NP synthesis.<sup>289</sup>

2. In co-flowing, the discrete and continuous phases are in a parallel manner and use either coaxial microchannel geometries or 3D configurations of tapered cylindrical capillaries that are inserted coaxially into rectangular or cylindrical capillaries. Investigation has been performed on the synthesis of Ag NPs in a coaxial flow reactor, finding that factors such as the flow rate of reagents and concentrations of trisodium citrate and silver nitrate played significant roles in reducing the NP size and dispersity, thereby affecting the resulting properties of the NPs.<sup>290</sup>

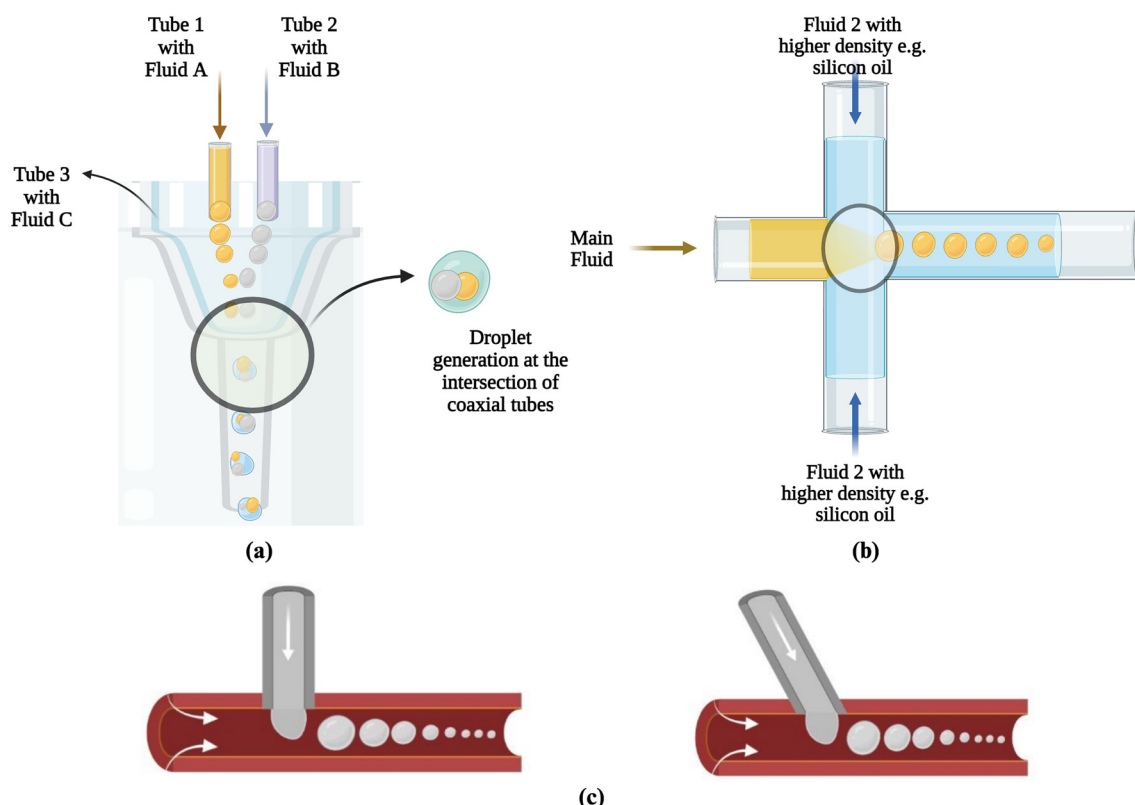


Fig. 11 a) Co axial tubes, b) hydrodynamic flow focusing, and c) cross-flow based droplet generation in microfluidic devices for NP synthesis.



3. In a focusing structure, the discrete phase is compressed into a thin stream surrounded by the continuous phase at the inlet intersection. At the downstream, due to interfacial instability, it subsequently breaks up into droplets.<sup>291,292</sup> Droplets have been used from flow-focusing structures for Au NP synthesis, and it found that NPs with smaller sizes can be synthesised compared to co-flowing and cross-flowing structures.<sup>293</sup>

## 5.2. Active microfluidics

External sources are involved in active microfluidic devices along with different channel geometries for NP synthesis. These external sources are mainly used to control the mixing of reagents that leads towards the generation of NPs with specific properties. In this section, six different types of active microfluidic devices have been discussed (Fig. 13). Table 5 summarises these six different active microfluidic approaches with some examples of synthesised NPs.

**5.2.1. Centrifugal microfluidics.** Centrifugal microfluidics use centrifugal force to accomplish different unit operations such as mixing, aliquoting and switching. In this type of microfluidic-based method, intrinsic forces play a vital role in the accomplishment of the process mechanism. Pseudo-forces are those inertial body forces acting on fluids or particles in rotating systems. In centrifugal microfluidics, they arise from the centripetal acceleration of the rotor and are, therefore, easily controllable. Pseudo-forces comprise the centrifugal force ( $F_c$ ), Coriolis force ( $F_{Co}$ ), and Euler force ( $F_E$ ).<sup>305</sup> Fig. 12a depicts different forces in such a kind of microfluidic system. With the help of these forces, parallel batch-type

microreactors can be constructed to synthesise multiple NPs on a single device. The simplicity and automatability of this approach can lead to high throughput NP synthesis. To better understand the process, normally, an imaging system is accompanied by the centrifugal stand. Fig. 12b shows a centrifugal microfluidic system with an integrated camera and light sources. A novel high-throughput synthetic platform was developed for producing diverse Au NPs using an innovative centrifugal microfluidic device and an automatic workstation, enabling 60 different reactions in a single run without human interference. The system efficiently varies NP morphologies *via* ascorbic acid dilution, optimizing for surface-enhanced Raman spectroscopy, while a portable workstation ensures an automated, cost-effective, and efficient NP synthesis process.<sup>306</sup> Centrifugal microfluidics are also employed for the synthesis of Pd–Au–Pt core–shell NPs. Leveraging unique microchannel design and passive valve structures, the platform can simultaneously perform 60 different reactions. By varying the ratio of Au to Pt in the catalyst, they showed that an Au/Pt ratio of 0.5 resulted in the most effective catalyst for  $H_2O_2$  production.<sup>307</sup>

**5.2.2. Pressure-driven microfluidics.** In these microfluidic devices, NP synthesis is achieved by controlling and enhancing mixing through pulsatile flows, distinct from passive methods. Unlike passive techniques, which rely on inherent properties like diffusion, capillary action, or gravity for fluid movement, this approach uses integrated planar micropumps to actively create pulsatile flow. These micropumps, acting as external pressure sources, generate rhythmic, pulsating fluid movements that effectively mix the components, a key factor in NP synthesis. This active method centred on pulsatile flows offers more precise control over fluid dynamics compared to passive

**Table 5** NP synthesis by different active microfluidic approaches

Active approach	Working principle	NP synthesised
Centrifugal microfluidics	Centrifugal force, along with other pseudo intrinsic forces <i>e.g.</i> Coriolis force and Euler force	Au NP-based colorimetric sensor for enantioselective detection of L-tryptophan <sup>294</sup> Cu hydride NPs for antitumor therapy <sup>295</sup>
Pressure microfluidics	Pulsatile flow with the help of micropumps and microvalves	Finger-operated pumping based microfluidic system for PLGA NP and liposome synthesis <sup>296</sup>
Thermal microfluidics	Thermal energy with the help of electrothermal effects, heat films and thermal bubbles	Microfluidic microreactor device with integrated heaters for temperature assisted synthesis of Au NPs <sup>297</sup> Ag NP-loaded alginate fibres for durable antibacterial application <sup>298</sup>
Electromagnetic microfluidics	Electromagnetic field by employing a permanent magnet, integrated electrodes, electromagnets and magnetic stirrers	Magnetic carbon dot (M-CD) NPs for intelligent fluorescence/colorimetric detection of tetracycline <sup>299</sup> Chiral plasmonic Au NPs for rapid cancer exosome isolation and analysis <sup>300</sup>
Acoustic microfluidics	Acoustic waves with the help of oscillatory microbubbles, sharp-edge structures, including oscillatory thin membranes, acoustic resonators, and acoustic metamaterials	Au NPs with the help of vibrating sharp-tip acoustic mixing <sup>301</sup>
Electrically-driven microfluidics	Electro-hydrodynamic (EHD), and electro-kinetic instability (EKI) with the methods <i>e.g.</i> electrophoresis, dielectrophoresis, and electroosmosis	Liposome NPs for cancer drug delivery <sup>302</sup> Chitosan NPs for effective oral drug delivery and bone tissue regeneration <sup>303</sup> Ag NPs for scalable nanofabrication and advanced functional coatings <sup>304</sup>



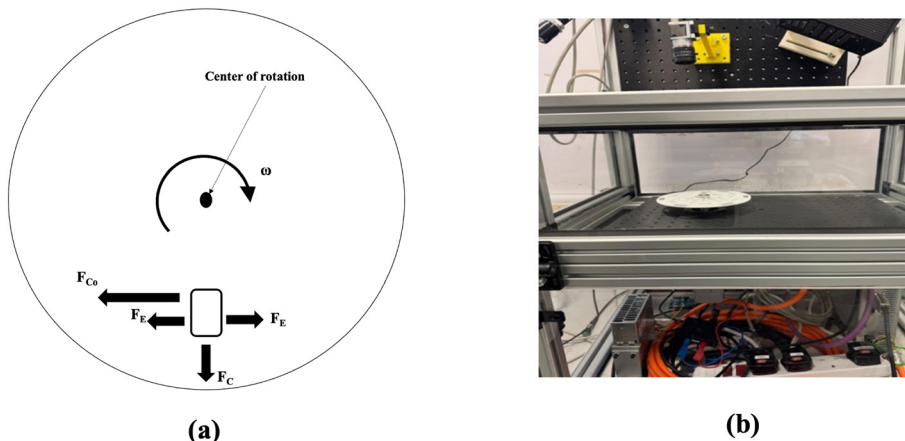


**Fig. 12** a) Pseudo-forces acting in centrifugal microfluidics. Centrifugal force ( $F_c$ ) always acts radially outward, the Coriolis force ( $F_{Co}$ ) acts perpendicular to both  $\omega$  and the fluid velocity and the Euler force ( $F_E$ ) is proportional to the angular acceleration. b) Centrifugal microfluidic system.

techniques.<sup>308</sup> This pulsatile flow assists in stretching and folding the fluid, resulting in a high mixing index in the microchannel.<sup>309</sup> Two micropumps have been employed to increase mixing which led to the generation of  $Fe_2O_3$  NPs within 15 minutes.<sup>310</sup> AuNPs are also been synthesized by coupling two piezoelectric valveless micropumps with a Y-shaped microchannel.<sup>311</sup> This type of microfluidic system provides a platform for very size-controlled NP synthesis. Software-based approaches have also been used to optimise pulsatile flow in pressure-driven micromixers.<sup>312</sup> Velocity pumping can also be

employed to disrupt the fluid flow and increase the contact area. Pulsatile pressure in microchannels can also be generated through a constant input of water head pressure.<sup>313</sup>

**5.2.3. Thermally-driven microfluidics.** Electrothermal effects,<sup>314</sup> thermal bubbles,<sup>315</sup> and increased diffusion coefficient<sup>316</sup> can be used to improve mixing by adding thermal energy. Alternative current-based electrothermal (ACET) effects, using staggered electrodes, have been used to enhance mixing in microfluidic chips. To optimise NP synthesis, a sequential micromixing platform has been

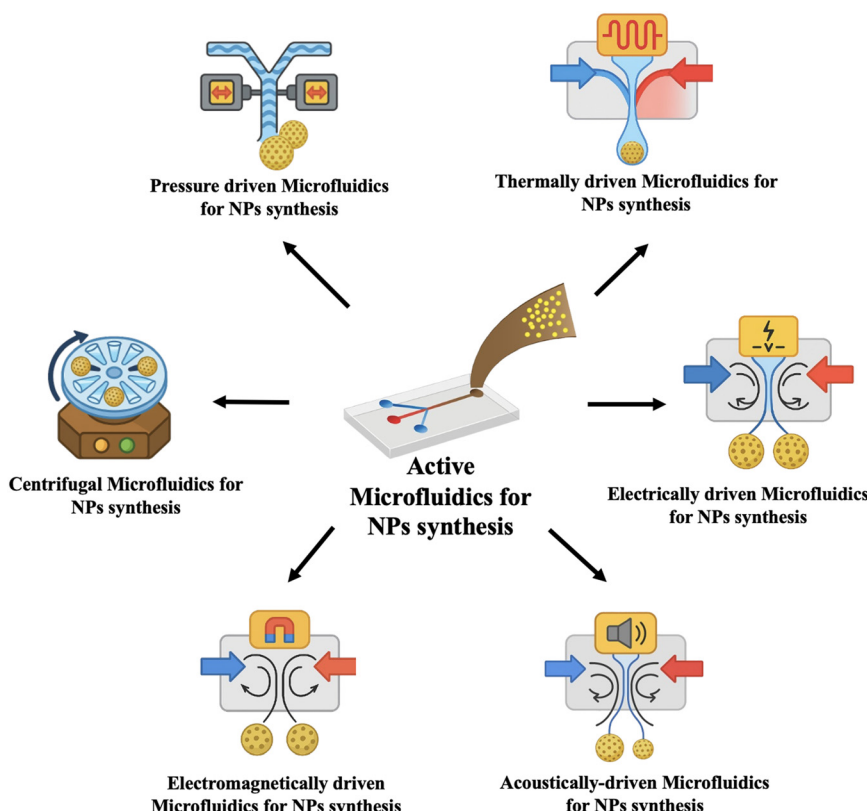


**Fig. 13** Schematic description of NP generation in different passive and active microfluidic devices.

developed using ACET. By adjusting the volume of each fluid and the AC voltage, they achieved a highly controlled synthesis process, resulting in NPs with improved dispersion, morphological control, and regular shapes. This method provided a promising alternative for complex chemical and biochemical reactions.<sup>317</sup> Film heaters at the base of microchannels can also be used in conjunction with alternating current (AC) electrodes, for further enhanced mixing efficiency. Experimental investigations have shown that combining film heaters with AC electrodes can lead to a mixing efficiency of 90%, compared to 87% mixing efficiency by internal Joule heat without film heaters.<sup>318</sup> AuNPs have been synthesized by integrating an induced graphene (LIG) heater with a microfluidic chip. The LIG heaters are thin, flexible and inexpensive and have shown a wide temperature range, reaching a maximum of 589 °C with 15% laser power and 5.5% scanning speed.<sup>319</sup> Recent research on thermally-driven microheaters indicates that asymmetrically placed microheaters result in significantly greater mixing due to secondary crossflow and asymmetric vortex created by the bubble collapse, compared to symmetrically arranged microheaters along the downstream of the centre plane of Y-micromixers.<sup>320</sup> Microheaters, along with thermal sensors, can also be fabricated inside microchannels by injecting conductive materials into the channels.<sup>321</sup>

**5.2.4. Electromagnetically driven microfluidics.** Magnetic field-based micromixers can be categorised into four types based on their working principles: (1) permanent magnet (PM), (2) integrated electrodes, (3) electromagnetic and (4) microstirrers. PM-based micromixers offer advantages such as flexible design, simple operating principles and the absence of special integration within microfluidic platforms. Mixing can also be enhanced by using a permanent magnet rotating with magnetic microbeads orbiting around NiFe discs. These orbiting microbeads result in fast mixing at low Re numbers.<sup>329</sup> However, there are certain drawbacks associated with PMs and electromagnets, as they tend to be bulky and generate harmful heating effects on biological samples. The usage of microfluidic devices consisting of two layers with microfabricated magnets can address these drawbacks.<sup>330</sup> Mixing efficiency of approx 99% can be achieved in the case of ferrofluid and deionised water by combining a uniform magnetic field with horizontally arranged microwires. Mixing is enhanced due to the introduction of eddies, whose impact is directly proportional to the number of microwires.<sup>331</sup> The mixing index also increases when the magnet is placed closer to the microchannel with a sinusoidal-shaped channel wall instead of straight channels.<sup>332</sup> Magnetic stirrers can also be used to enhance mixing, particularly with fluids that exhibit viscosities at low rotational velocities.<sup>333</sup> Magnetically actuated cilia, which typically consist of superparamagnetic or ferromagnetic particles dispersed in magnetically non-activated materials such as PDMS, also contribute to enhancing the mixing.<sup>334,335</sup> Recently, shape-programable cilia have been introduced in microfluidics, demonstrating

excellent improvement in mixing efficiency.<sup>336</sup> Magnetic microneedles in microchannels have been used for the synthesis of chitosan NPs. Magnetic microactuators in a PDMS microfluidic chip placed on a magnetic stirrer have been used to increase mixing efficiency for the synthesis of penicillin-loaded titanium oxide NPs.<sup>337</sup>

**5.2.5. Acoustically-driven microfluidics.** Acoustofluidics, which combines microfluidics and acoustics, is an emerging research field with a wide range of applications. Acoustic streaming in a microfluidic disc is induced by the interaction between the solid and fluid in the viscous flow, resulting in time-averaged nonlinear dynamics.<sup>338,339</sup> Acoustic streaming offers unique benefits, as it can be manipulated with six degrees of freedom, making it versatile.<sup>340</sup> Additionally, due to its contactless nature, it is considered biocompatible.<sup>341</sup> Acoustic streaming can be highly precise, as waves can be applied in a highly controllable manner. Various mechanisms can be used to generate acoustic streaming. Microbubbles can be energised by applying acoustic waves, and the mixing time is directly proportional to the number of energised bubbles.<sup>342</sup> Oscillatory microbubbles can generate microstreaming vortices, which can be used to increase mixing in microchannels at very low Re numbers.<sup>343</sup> The resonance frequency ( $F$ ) can be applied to actuate the microbubble increases as the bubble size decreases.<sup>344</sup> Sharp-edge structures, including oscillatory thin membranes, can be used to generate an acoustic field similar to microbubbles, enhancing mixing and pumping along the microchannels.<sup>345</sup> Rapid mixing for the synthesis of organic NPs has been achieved using acoustic streaming at the boundaries by coupling the energised bubbles with sharp edges.<sup>346</sup> A silicon-based oscillator positioned between two microchannels has been used to generate DNA NPs.<sup>347</sup> PLGA-PEG NPs have been synthesised by using acoustofluidic discs and demonstrated that high throughput, small size, and uniformity are achieved as compared to the conventional vortex-based microfluidic device.<sup>348</sup>

**5.2.6. Electrically-driven microfluidics.** Electrically-driven micromixers are based on the principles of electro-hydrodynamics (EHD)<sup>349</sup> and electro-kinetic instability (EKI).<sup>350</sup> These micromixers use sources of AC or DC to mobilise electrically charged fluid and disturb the fluidic interface.<sup>350</sup> Methods such as electrophoresis,<sup>351</sup> electroosmosis,<sup>352</sup> and dielectrophoresis<sup>353</sup> may be used in such types of micromixers. An external electric field is applied to generate electro-thermal vortices, which increase mixing efficiency by enhancing convective diffusion.<sup>354</sup> DC voltage has also been used to generate in-plane vortices, resulting in improved mixing efficiency.<sup>355</sup> EHD microfluidic devices based on the nanoprecipitation process have been proven highly efficient for NP synthesis.<sup>356</sup> Electrophoresis, which is the movement of non-conductive and conductive particles in response to an external electrical field applied to an electrolyte solution, can be used to increase mixing rates. The use of conductive particles in the presence of a circular conductive particle and an applied external electric field

induces vortices around the particle, enhancing mixing.<sup>357</sup> Electroosmotic flow can also be used for efficient mixing in microfluidic devices as it effectively pumps fluids without the need for additional mechanical pumping mechanisms.<sup>352</sup> Electroosmotic micromixers have successfully synthesised gold NPs.<sup>358</sup>

Dielectrophoresis is the movement of neutral particles caused by an AC electric field. Bilateral motion of particles occurs due to the formation of a dipole moment between electrodes, resulting in stretching and folding of fluids and chaotic advection, thereby increasing the mixing index. Similar to electrophoresis-based micromixers, dielectrophoresis-based micromixers can employ conductive particles to enhance mixing.

#### Recent advancement in microfluidics for NP synthesis

**3D printed microfluidics.** The convergence of 3D printing and microfluidic technologies has opened new frontiers in the controlled synthesis of NPs. These 3D printed microfluidic chips enabled the production of liposome MPs with tunable sizes and high stability by optimizing flow parameters such as the total flow rate and flow rate ratio.<sup>359</sup> 3D printed microreactors were also integrated with a UV-vis diagnostic system. It enabled droplet-based, high-throughput screening of Au nanoparticle synthesis. This system analysed over 1000 droplets in under an hour, demonstrating how 3D printed setups can rapidly optimize synthesis conditions through automation and multivariate analysis.<sup>360</sup>

Further advancing the field, hybrid systems combining 3D printing with micromilling techniques were established. It has enabled the design of impinging jet reactors (FIJRs) which offer superior mixing, temperature control, and scalability. These platforms have successfully produced colloidal Ag and FeO NPs with controlled sizes during continuous operation, highlighting their robustness and fouling resistance.<sup>361</sup> Moreover, microfluidic chips fabricated for drug-loaded polymeric NP synthesis such as PLGA loaded with pentamidine demonstrated the potential of 3D printed systems to precisely tune formulation characteristics for biomedical applications. By adjusting flow rates and surfactant concentrations, researchers achieved monodisperse nanoparticles with therapeutic relevance and consistent performance.<sup>362</sup>

Altogether, these examples underscore the growing role of 3D printed microfluidic systems as versatile, scalable, and high-precision tools for nanoparticle synthesis in both industrial and biomedical domains (Table 6).

**Modular microfluidics.** Modular microfluidic systems have emerged as a transformative platform for the precise and scalable synthesis of NPs. Their small reaction volumes and excellent control over fluid dynamics enable highly tunable reaction environments, particularly useful in the production of functional nanomaterials. Recent advancements have shown the strength of microfluidics in fabricating metal nano-electrocatalysts with tailored morphologies and electrochemical properties, offering better control over nucleation, growth, and reaction enhancement mechanisms.<sup>363</sup> These systems allow for efficient parameter optimization, real-time control, and continuous operation key features for ensuring reproducibility and structural precision in nanoparticle production. The modularity of microfluidic setups further supports easy integration and reconfiguration of components, making them suitable for adapting to various synthesis protocols.

In drug delivery, modular microfluidics has proven equally impactful. Hydrodynamic focusing within continuous-flow microfluidic chips, such as PLA-based devices, enables the single-step synthesis of lipid nanoparticles under uniform conditions, resulting in consistent particle sizes ( $\leq 200$  nm) ideal for biomedical applications.<sup>364</sup> This streamlined approach not only enhances efficiency but also supports rapid parameter screening for formulation development. Additionally, microfluidic cartridge-based mixers (MCF) have enabled scalable and purification-free layer-by-layer (LbL) surface modification of NPs, essential for targeted and controlled drug delivery. These modular systems facilitate robust electrostatic assembly on diverse NP cores without the need for excess materials or laborious post-processing.<sup>365</sup> Overall, modular microfluidic systems stand out as powerful, flexible, and scalable platforms for engineering next-generation nanoparticles across both therapeutic and catalytic domains (Table 6).

**Intelligent microfluidics.** Intelligent microfluidics has emerged as an advanced approach for the design and

Table 6 Advanced and hybrid microfluidic systems

Microfluidic technologies	NPs synthesised
3D printed microfluidics	Ag NPs synthesized through high throughput continuous flow using a 3D helical microfluidic chip for enhanced flow-boiling heat transfer in electronic chip <sup>322</sup> Liposomal NPs synthesized for drug delivery applications using UV LCD 3D-printed microfluidic chips <sup>323</sup>
Modular microfluidics	Si NPs synthesized for photonic crystal applications <sup>324</sup> PLGA nanoparticles (33–180 nm) synthesized for drug and vaccine delivery using a low-cost, modular capillary-based microfluidic system <sup>325</sup>
Intelligent microfluidics	Coupling of machine learning with microfluidics for NP synthesis using RSM-differential evolution and RSM-NSGA-II enabled multi-objective optimization of micromixer design for enhanced mixing efficiency and energy reduction <sup>326</sup> Intelligent microfluidics for PLGA nanoparticle synthesis using TGAN-augmented datasets and predictive models such as decision tree, random forest, and deep neural networks enabled accurate NP size prediction and identification of key synthesis parameters <sup>327</sup> Au NPs synthesized for multiplexed point-of-care detection of cysteamine using an AI-enhanced lab-on-a-disc (AI-LOAD) system <sup>328</sup>



synthesis of NPs by leveraging artificial intelligence (AI), machine learning (ML), and computational modeling (Table 6). This integration of AI techniques into microfluidic platforms allows enhanced control over NP characteristics such as size, shape, surface charge, drug loading and release efficiency parameters critical for applications in drug delivery, biosensing, gene therapy, and diagnostics.

Recent advances include the application of data-driven surrogate modelling and multi-objective optimization to refine micromixer geometries, leading to more energy-efficient NP synthesis. These systems have demonstrated over 80% reduction in pressure drop and a 20% improvement in mixing efficiency at low Reynolds numbers, significantly improving the scalability and reproducibility of particle fabrication for hydrogel engineering and therapeutic delivery systems.<sup>326</sup>

Machine learning algorithms—such as decision trees, random forests, and deep neural networks—have been employed for predicting and tuning the properties of polymeric NPs. PLGA NPs have been modelled to achieve high prediction accuracy in particle size and zeta potential, with ensemble models like BAG-SVR and BAG-PR outperforming traditional regressors.<sup>327,366</sup>

The convergence of AI with microfluidics is further evident in the development of systems which integrates experimental microfluidic data with random forest models to predict nanomedicine attributes, including hydrodynamic diameter, polydispersity index, and encapsulation efficiency. This framework accelerates formulation development by enabling user-defined design of NP systems.<sup>367</sup> Similarly, inverse modelling combined with Latin hypercube sampling and data assimilation has been successfully applied to the synthesis of Ag nanoparticles, facilitating precise control over size prediction and hydrodynamic conditions in microfluidic environments.<sup>367</sup>

The potential of intelligent microfluidics also extends into diagnostic platforms. The AI-enhanced lab-on-a-disc (AI-LOAD) system exemplifies this innovation, utilizing Au nanoparticles and ML-based pattern recognition to enable multiplexed, rapid colorimetric detection of cysteamine and structurally similar biothiols from minimal whole blood volumes.<sup>328</sup> The integration of AI and additive manufacturing has enabled real-time tracking of droplets in droplet microfluidics by AI-assisted fluid simulations, and the fabrication of complex three-dimensional microfluidic architectures. This leads towards more accurate modeling of multiphase flows and designing more efficient microfluidic devices.<sup>368</sup>

Moreover, AI-assisted formulation strategies are advancing the design of smart, stimuli-responsive polymeric NPs capable of controlled and targeted drug release. These innovations, rooted in modern polymer chemistry and enabled by predictive modelling, offer new opportunities for personalized nanomedicine.<sup>369</sup>

## 6. Current challenges and future prospects

Although microfluidic platforms provide a superior alternative for NP synthesis, there are still a few challenges

that need to be addressed to make microfluidic-based NP synthesis more efficient. These challenges range from the usage of the conventional world to chip connectors for connectivity of microfluidic devices with the reagents' reservoirs and tubing to the automation of the whole synthesis process based on machine learning-based predictive models. Further research in microfluidic systems aims to automate testing, reduce user intervention to minimise human error and increase NP replicability in production.

Microfluidic platforms are primarily operated manually, but there is a growing trend towards coupling microfluidics with machine learning and optical probing. This integration holds the potential for intelligent microfluidic devices, revolutionising nanomaterials, drug discovery, and developmental biology. Integration of microfluidics with artificial intelligence can be a breakthrough in the field of NP synthesis with highly controlled desired properties. As evident from the literature, controllable synthesis of NPs is an area of great research interest, and this can enhance the application of NPs, especially in the field of smart drug delivery systems. To improve NP synthesis in microfluidics, there is a need to investigate further the impact of mixing parameters in microchannels on the properties of NPs. More control during the mixing can easily lead towards better control of NP properties. Machine learning has been coupled with microfluidic based synthesis of PLGA NPs to study the influence of different reaction parameters.<sup>370</sup> PLGA NP production has also been optimized by combining design of experiment and machine learning.<sup>371</sup> A tabular generative adversarial network has also been employed to predict NP size in microfluidics.<sup>327</sup> These machine learning based predictive models for NP properties have laid the foundation for online sensing and automation of microfluidic based NP production.

The widespread adoption of microfluidic devices has been hindered by the high-cost and single-use nature of microfluidic connectors. Different researchers have introduced a variety of different types of microfluidic connectors to address these challenges.<sup>372,373</sup> Universal and versatile magnetic microfluidic connectors have also been introduced.<sup>374</sup> Along with magnetic connectors, fast plug and play mechanical connectors have also been developed for efficient connections.<sup>375</sup> Other than connecting the microfluidic devices with the reservoir syringes, the overall handling and use of microfluidic devices with such small dimensions is also not an easy task. The micrometric scale size of microchannels makes it difficult to clean channels and often leads towards clogging. For instance, there are not enough suitable standards for microfluidic accessories, such as connectors, micropumps, and microvalves. This leads to issues such as misalignment, blockage, leakage, degradation, and dimensional errors. Furthermore, accurate methods for real-time flow rate fluctuation measurement, specifically for passive microfluidic devices where flow rate is critical, are lacking. This additional equipment, such as temperature



sensors, ultrasound systems, magnetic fields and automated syringe pumps, adds an extra cost to the microfluidic-based NP synthesis system. Scalability of NP synthesis through microfluidics is also the main industrial challenge. These systems are typically characterised by very small reaction volumes and low flow rates, which results in very limited NP throughput. Complex fluid dynamics and control systems involved in microfluidic devices can be difficult to replicate and maintain while working with large volumes. Integrating microfluidic systems into existing pharmaceutical manufacturing processes and infrastructures can also be very challenging. Adapting and aligning this technology with current NP synthesis systems, quality control standards, and regulatory requirements may require significant modifications to the production setup and additional validation.<sup>376</sup>

Different strategies have been used to overcome this challenge for scaling up the NP synthesis in microfluidics. Scaled-up synthesis of hollow Au NPs using both batch and microfluidic approaches has been investigated. It has been found that the microfluidic approach offers a 10-fold increase in the throughput of hollow Au NPs with the same desirable features by increasing the diameter and length of the microchannels.<sup>377</sup> A more appealing and practical approach, rather than increasing channel size, which can impair heat and mass transfer, is parallelisation, where multiple microfluidic reactors are operated simultaneously on a single microfluidic chip. A scalable parallelised microfluidic device featuring an array of 128 mixing channels was employed for lipid-based NPs. This innovative device incorporated an array of staggered herringbone micromixer channels and flow resistors to operate simultaneously. This approach resulted in a 100-fold throughput of lipid-based NPs compared to single microfluidic channels without compromising the desired properties of the lipid-based NPs.<sup>378</sup> In recent years, there has been a significant increase in potential microfluidic devices, as reflected in the rising number of patent submissions to the US Food and Drug Administration. However, the lack of regulation and standardisation in microfluidic-based platform design has impeded the commercial success of these devices.

This gap has created a strong demand for universally accessible tools and software to evaluate microfluidic devices consistently. The microfluidic research community faces the challenge of establishing well-defined standards, which are essential for facilitating communication among various microfluidic professionals (*i.e.*, academics, researchers, and industry) throughout different stages of product development. Addressing this challenge is crucial for mitigating a wide range of problems.

Overall, microfluidic technology revolutionises NP synthesis by overcoming the limitations of conventional methods—reducing sample loss, streamlining lengthy procedures, and eliminating the need for costly, multi-step equipment. By enabling precise control over NP characteristics, microfluidic platforms pave the way for highly

efficient and targeted drug delivery systems, setting new standards in biomedical applications.

## Data availability

No primary research results, software or code have been included and no new data were generated or analysed as part of this review.

## Conflicts of interest

There are no conflicts to declare.

## Acknowledgements

This publication has emanated from research conducted with the financial support of Taighde Éireann – Research Ireland under Grant number 18/CRT/6183. For the purpose of Open Access, the author has applied a CC BY public copyright licence to any Author Accepted Manuscript version arising from this submission. Fig. 2 Created in BioRender. Saeed, M. (2025) <https://BioRender.com/ob25b1x>. Fig. 3 Created in BioRender. Saeed, M. (2025) <https://BioRender.com/tscjlbw>. Fig. 4 Created in BioRender. Saeed, M. (2025) <https://BioRender.com/beijyjn>. Fig. 5 Created in BioRender. Saeed, M. (2025) <https://BioRender.com/ajcyh5m>. Fig. 6 Created in BioRender. Saeed, M. (2025) <https://BioRender.com/kmfnokr>. Fig. 8a-c Created in BioRender. Saeed, M. (2025) <https://BioRender.com/3fez1ct>. Fig. 11 Created in BioRender. Saeed, M. (2025) <https://BioRender.com/p0ro0hg>.

## References

- 1 V. Mohanraj and Y. Chen, Nanoparticles-a review, *Trop. J. Pharm. Res.*, 2006, **5**(1), 561–573.
- 2 S. Vijayaram, *et al.*, Applications of green synthesized metal nanoparticles—a review, *Biol. Trace Elem. Res.*, 2024, **202**(1), 360–386.
- 3 F. Eker, *et al.*, A comprehensive review of nanoparticles: from classification to application and toxicity, *Molecules*, 2024, **29**(15), 3482.
- 4 Q. Liu, J. Guan, R. Song, X. Zhang and S. Mao, Physicochemical properties of nanoparticles affecting their fate and the physiological function of pulmonary surfactants, *Acta Biomater.*, 2022, **140**, 76–87.
- 5 H. Ebadi-Dehaghani and M. Nazempour, *Thermal Conductivity of Nanoparticles Filled Polymers*, INTECH Open Access Publisher, 2012.
- 6 Y. Geng, *et al.*, A comprehensive presentation on nanoparticles electrical conductivity of nanofluids: Statistical study concerned effects of temperature, nanoparticles type and solid volume concentration, *Phys. A*, 2020, **542**, 123432.
- 7 Z. Qiao, H. Feng and J. Zhou, Molecular dynamics simulations on the melting of gold nanoparticles, *Phase Transitions*, 2014, **87**(1), 59–70.
- 8 S. Alavi and D. L. Thompson, Molecular dynamics simulations of the melting of aluminum nanoparticles, *J. Phys. Chem. A*, 2006, **110**(4), 1518–1523.



9 S. Kim, *et al.*, Effects of nanoparticle deposition on surface wettability influencing boiling heat transfer in nanofluids, *Appl. Phys. Lett.*, 2006, **89**(15), 153107.

10 L. Gloag, *et al.*, Advances in the application of magnetic nanoparticles for sensing, *Adv. Mater.*, 2019, **31**(48), 1904385.

11 P. Suchomel, *et al.*, Simple size-controlled synthesis of Au nanoparticles and their size-dependent catalytic activity, *Sci. Rep.*, 2018, **8**(1), 1–11.

12 K. Naim, *et al.*, Supramolecular confinement within chitosan nanocomposites enhances singlet oxygen generation, *ChemPlusChem*, 2018, **83**(5), 418–422.

13 P. Yu, *et al.*, Effects of plasmonic metal core-dielectric shell nanoparticles on the broadband light absorption enhancement in thin film solar cells, *Sci. Rep.*, 2017, **7**(1), 1–10.

14 P. M. Carvalho, *et al.*, Application of light scattering techniques to nanoparticle characterization and development, *Front. Chem.*, 2018, **6**, 237.

15 I. Khan, K. Saeed and I. Khan, Nanoparticles: properties, applications and toxicities, *Arabian J. Chem.*, 2019, **12**, 908–931.

16 J. Jeevanandam, *et al.*, Review on nanoparticles and nanostructured materials: history, sources, toxicity and regulations, *Beilstein J. Nanotechnol.*, 2018, **9**(1), 1050–1074.

17 N. A. Lopes and A. Brandelli, Nanostructures for delivery of natural antimicrobials in food, *Crit. Rev. Food Sci. Nutr.*, 2018, **58**(13), 2202–2212.

18 S. Mehraji and D. L. DeVoe, Microfluidic synthesis of lipid-based nanoparticles for drug delivery: Recent advances and opportunities, *Lab Chip*, 2024, **24**(5), 1154–1174.

19 N. Rajput, Methods of preparation of nanoparticles-a review, *Int. J. Adv. Eng. Technol.*, 2015, **7**(6), 1806.

20 S. Hasan, A review on nanoparticles: their synthesis and types, *Res. J. Recent Sci.*, 2015, **2277**, 2502.

21 S. A. M. Ealia and M. P. Saravanakumar, A review on the classification, characterisation, synthesis of nanoparticles and their application, *IOP Conf. Ser.: Mater. Sci. Eng.*, 2017, **263**(3), 032019.

22 W. H. De Jong and P. J. Borm, Drug delivery and nanoparticles: applications and hazards, *Int. J. Nanomed.*, 2008, **3**(2), 133–149.

23 E. Chiesa, R. Dorati, S. Pisani, B. Conti, G. Bergamini, T. Modena and I. Genta, The microfluidic technique and the manufacturing of polysaccharide nanoparticles, *Pharmaceutics*, 2018, **10**(4), 267.

24 R. Abedini-Nassab, M. Pouryosef Miandoab and M. Şaşmaz, Microfluidic synthesis, control, and sensing of magnetic nanoparticles: A review, *Micromachines*, 2021, **12**(7), 768.

25 S. Hettiarachchi, H. Cha, L. Ouyang, A. Mudugamuwa, H. An, G. Kijanka, N. Kashaninejad, N. T. Nguyen and J. Zhang, Recent microfluidic advances in submicron to nanoparticle manipulation and separation, *Lab Chip*, 2023, **23**(5), 982–1010.

26 A. Fabozzi, F. Della Sala, M. di Gennaro, M. Barretta, G. Longobardo, N. Solimando, M. Pagliuca and A. Borzacchiello, Design of functional nanoparticles by microfluidic platforms as advanced drug delivery systems for cancer therapy, *Lab Chip*, 2023, **23**(5), 1389–1409.

27 Y. Liu, G. Yang, Y. Hui, S. Ranaweera and C. X. Zhao, Microfluidic nanoparticles for drug delivery, *Small*, 2022, **18**(36), 2106580.

28 A. Meher, A. Tandi, S. Moharana, S. Chakraborty, S. S. Mohapatra, A. Mondal, S. Dey and P. Chandra, Silver nanoparticle for biomedical applications: A review. *Hybrid, Advances*, 2024, 100184.

29 B. Mishra Sunil, K. S. S. Liyakat and K. K. S. Liyakat, Nanotechnology's Importance in Mechanical Engineering, *Development*, 2024, **4**, 5.

30 S. S. Rout and K. C. Pradhan, A review on antimicrobial nano-based edible packaging: Sustainable applications and emerging trends in food industry, *Food Control*, 2024, 11047.

31 M. M. Ghobashy, S. A. Alkhursani, H. A. Alqahtani, T. K. El-damhougy and M. Madani, Gold nanoparticles in microelectronics advancements and biomedical applications, *Mater. Sci. Eng., B*, 2024, **301**, 117191.

32 D. S. Chaudhari, R. P. Upadhyay, G. Y. Shinde, M. B. Gawande, J. Filip, R. S. Varma and R. Zboril, A review on sustainable iron oxide nanoparticles: synthesis and application in organic catalysis and environmental remediation, *Green Chem.*, 2024, **2024**(26), 7579–7655.

33 S. Singh, H. Tiwari, A. Verma, P. Gupta, A. Chattopadhyaya, A. Singh, S. Singh, B. Kumar, A. Mandal, R. Kumar and A. K. Yadav, Sustainable synthesis of novel green-based nanoparticles for therapeutic interventions and environmental remediation, *ACS Synth. Biol.*, 2024, **13**(7), 1994–2007.

34 W. Hussain, S. Algarni, G. Rasool, H. Shahzad, M. Abbas, T. Alqahtani and K. Irshad, Advances in nanoparticle-enhanced thermoelectric materials from synthesis to energy harvesting: a review, *ACS Omega*, 2024, **9**(10), 11081–11109.

35 B. Monteiro and S. Simões, Recent Advances in Hybrid Nanocomposites for Aerospace Applications, *Metals*, 2024, **14**(11), 1283.

36 P. Biehl, M. Von der Lühe, S. Dutz and F. H. Schacher, Synthesis, characterization, and applications of magnetic nanoparticles featuring polyzwitterionic coatings, *Polymers*, 2018, **10**(1), 91.

37 A. M. ElSawy, N. F. Attia, H. I. Mohamed, M. Mohsen and M. H. Talaat, Innovative coating based on graphene and their decorated nanoparticles for medical stent applications, *Mater. Sci. Eng., C*, 2019, **96**, 708–715.

38 A. Singh, P. Chauhan and T. G. Mamatha, A review on tribological performance of lubricants with nanoparticles additives, *Mater. Today: Proc.*, 2020, **25**, 586–591.

39 W. Yang, M. Rallini, M. Natali, J. Kenny, P. Ma, W. Dong, L. Torre and D. Puglia, Preparation and properties of adhesives based on phenolic resin containing lignin micro and nanoparticles: A comparative study, *Mater. Des.*, 2019, **161**, 55–63.

40 J. R. Xavier, Improvement in corrosion resistance and mechanical properties of epoxy coatings on steel with the addition of thiadiazole treated ZrC, *J. Mater. Eng. Perform.*, 2023, **32**(9), 3980–3994.



41 S. S. Selvan and I. R. Vedaraj, Effects of nanoparticles on the mechanical and thermal behavior of fiber reinforced polymer composites-A review, *Mater. Today: Proc.*, 2023, DOI: [10.1016/j.matpr.2023.07.008](https://doi.org/10.1016/j.matpr.2023.07.008).

42 N. H. Khday, B. T. Almuarqab and G. El Enany, Nanoparticle-embedded polymers and their applications: a review, *Membranes*, 2023, **13**(5), 537.

43 M. Kot, L. Major, J. M. Lackner, K. Chronowska-Przywara, M. Janusz and W. Rakowski, Mechanical and Tribological Properties of Carbon-Based Graded Coatings, *J. Nanomater.*, 2016, **2016**(1), 8306345.

44 S. Mallakpour and F. Sorous, Surface coating of  $\alpha$ -Al<sub>2</sub>O<sub>3</sub> nanoparticles with poly (vinyl alcohol) as biocompatible coupling agent for improving properties of bio-active poly (amide-imide) based nanocomposites having l-phenylalanine linkages, *Prog. Org. Coat.*, 2015, **85**, 138–145.

45 W. Shao, D. Nabb, N. Renevier, I. Sherrington, Y. Fu and J. Luo, Mechanical and anti-corrosion properties of TiO<sub>2</sub> nanoparticle reinforced Ni coating by electrodeposition, *J. Electrochem. Soc.*, 2012, **159**(11), D671.

46 A. M. Brindhav, S. Sharma, S. Azizi and V. S. Rana, Unveiling the Cutting-edge Applications of Nanotechnology in the Food Industry-From Lab to Table-a comprehensive review, *J. Agric. Food Res.*, 2025, 1018.

47 Q. Gao, Z. Feng, J. Wang, F. Zhao, C. Li and J. Ju, Application of nano-ZnO in the food preservation industry: antibacterial mechanisms, influencing factors, intelligent packaging, preservation film and safety, *Crit. Rev. Food Sci. Nutr.*, 2024, 1–27.

48 H. G. El Gohary, I. A. Alhagri, T. F. Qahtan, A. N. Al-Hakimi, A. Saeed, F. Abolaban, E. M. Alshammari and G. M. Asnag, Reinforcement of structural, thermal and electrical properties and antibacterial activity of PVA/SA blend filled with hybrid nanoparticles (Ag and TiO<sub>2</sub> NPs): Nanodielectric for energy storage and food packaging industries, *Ceram. Int.*, 2023, **49**(12), 20174–20184.

49 R. P. Mahato, P. Singh and S. Srivastava, Prospects and Challenges of Nanofilms-based Edible Food Coatings for Enhancement of Their Shelf Life, in *The Nanotechnology Driven Agriculture*, 2024, pp. 204–224.

50 N. Hossain, M. H. Mobarak, M. A. Mimona, M. A. Islam, A. Hossain, F. T. Zohura and M. A. Chowdhury, Advances and significances of nanoparticles in semiconductor applications-A review, *Results Eng.*, 2023, **19**, 101347.

51 S. Nazir, J. M. Zhang, M. Junaid, S. Saleem, A. Ali, A. Ullah and S. Khan, Metal-based nanoparticles: basics, types, fabrications and their electronic applications, *Z. Phys. Chem.*, 2024, **238**(6), 965–995.

52 A. Bobsin, T. C. Rodrigues, I. J. Fernandes, S. B. Ferreira, C. R. Peter, W. Hasenkamp and C. A. Moraes, Copper and silver microparticles for high-performance conductive inks in electronic chip shielding, *Mater. Chem. Phys.*, 2024, **315**, 129007.

53 L. Wang, F. Xia, W. Xu, G. Wang, S. Hong, F. Cheng, B. Wu and N. Zheng, Antioxidant High-Conductivity Copper Pastes Based on Core-Shell Copper Nanoparticles for Flexible Printed Electronics, *Adv. Funct. Mater.*, 2023, **33**(26), 2215127.

54 M. Ba, S. Mansouri, A. Jouili, Y. Yousfi, L. Chouiref, M. Jdir, M. Erouel, F. Yakuphanoglu and L. E. Mir, Controlling of hysteresis by varying ZnO-nanoparticles amount in P3HT: ZnO hybrid thin-film transistor: modeling, *J. Electron. Mater.*, 2023, **52**(2), 1203–1215.

55 Z. T. Zhang, Y. X. Dong and B. Y. Cao, Promoting temperature control and energy conservation by smart thermal management using nanoparticle suspensions with tunable thermal conductivity, *Appl. Energy*, 2024, **374**, 124097.

56 D. Kirubakaran, J. B. A. Wahid, N. Karmegam, R. Jeevika, L. Sellapillai, M. Rajkumar and K. J. SenthilKumar, A comprehensive review on the green synthesis of nanoparticles: advancements in biomedical and environmental applications, *Biomed. Mater. & Devices*, 2025, 1–26.

57 Y. Sun, Y. Jiang, H. Wei, Z. Zhang, S. Irshad, X. Liu, Y. Xie, Y. Rui and P. Zhang, Nano-enabled strategies for greenhouse gases emission mitigation: a comprehensive review, *Nano Today*, 2024, **57**, 102378.

58 N. K. Das, S. Veeralingam and S. Badhulika, Zinc ferrite nanoparticle-based wearable piezoelectric nanogenerators as self-powered sensors to monitor human motion, *ACS Appl. Nano Mater.*, 2023, **6**(14), 13431–13442.

59 A. Fereydooni, C. Yue and Y. Chao, A Brief Overview of Silicon Nanoparticles as Anode Material: A Transition from Lithium-Ion to Sodium-Ion Batteries, *Small*, 2024, **20**(17), 2307275.

60 N. Rashidi, M. Davidson, V. Apostolopoulos and K. Nurgali, Nanoparticles in cancer diagnosis and treatment: Progress, challenges, and opportunities, *J. Drug Delivery Sci. Technol.*, 2024, 105599.

61 S. Wang, *et al.*, Fe<sup>2+</sup>-Dominated Relaxometric Properties of Iron Oxide Nanoparticles as MRI Contrast Agents, *J. Phys. Chem. Lett.*, 2024, **15**(34), 8861–8866.

62 M. A. Beach, U. Nayanathara, Y. Gao, C. Zhang, Y. Xiong, Y. Wang and G. K. Such, Polymeric nanoparticles for drug delivery, *Chem. Rev.*, 2024, **124**(9), 5505–5616.

63 V. Rahimkhoei, *et al.*, Advances in inorganic nanoparticles-based drug delivery in targeted breast cancer theranostics, *Adv. Colloid Interface Sci.*, 2024, 103204.

64 S. M. Naghib, *et al.*, Chitosan-based smart stimuli-responsive nanoparticles for gene delivery and gene therapy: Recent progresses on cancer therapy, *Int. J. Biol. Macromol.*, 2024, 134542.

65 C. M. Jogdeo, *et al.*, Beyond lipids: exploring advances in polymeric gene delivery in the lipid nanoparticles era, *Adv. Mater.*, 2024, **36**(31), 2404608.

66 X. Gu and T. Minko, Targeted nanoparticle-based diagnostic and treatment options for pancreatic cancer, *Cancers*, 2024, **16**(8), 1589.

67 L. L. Panigrahi, *et al.*, Nanoparticle-mediated diagnosis, treatment, and prevention of breast cancer, *Nanoscale Adv.*, 2024, **6**(15), 3699–3713.

68 Y. Guan, *et al.*, Nanoparticles and bone microenvironment: a comprehensive review for malignant bone tumor diagnosis and treatment, *Mol. Cancer*, 2024, **23**(1), 246.

69 T. Aili, *et al.*, Recent advances of self-assembled nanoparticles in the diagnosis and treatment of atherosclerosis, *Theranostics*, 2024, **14**(19), 7505.



70 Q. Zhang, *et al.*, Renal clearable magnetic nanoparticles for magnetic resonance imaging and guided therapy, *Wiley Interdiscip. Rev.: Nanomed. Nanobiotechnol.*, 2024, **16**(1), e1929.

71 L. Wen, *et al.*, Tailoring zinc ferrite nanoparticle surface coating for macrophage-affinity magnetic resonance imaging of atherosclerosis, *ACS Appl. Mater. Interfaces*, 2024, **16**(11), 13496–13508.

72 I. Waheed, *et al.*, Lipid-based nanoparticles as drug delivery carriers for cancer therapy, *Front. Oncol.*, 2024, **14**, 1296091.

73 P. Kesharwani, *et al.*,  $\alpha v\beta 3$  integrin targeting RGD peptide-based nanoparticles as an effective strategy for selective drug delivery to tumor microenvironment, *J. Drug Delivery Sci. Technol.*, 2024, 105663.

74 L. Sonowal and S. Gautam, Advancements and challenges in carbon nanotube-based drug delivery systems, *Nano-Struct. Nano-Objects*, 2024, **38**, 101117.

75 M. H. Karami, M. Abdouss and B. Maleki, The state of the art metal nanoparticles in drug delivery systems: A comprehensive review, *Nanomed. J.*, 2024, **11**(3), 222–249.

76 Y. Dang and J. Guan, Nanoparticle-based drug delivery systems for cancer therapy, *Smart Mater. Med.*, 2020, **1**, 10–19.

77 J. Dai, M. Ashrafizadeh, A. R. Aref, G. Sethi and Y. N. Ertas, Peptide-functionalized-assembled and-loaded nanoparticles in cancer therapy, *Drug Discovery Today*, 2024, 103981.

78 X. Huang, T. He, X. Liang, Z. Xiang, C. Liu, S. Zhou, R. Luo, L. Bai, X. Kou, X. Li and R. Wu, Advances and applications of nanoparticles in cancer therapy, *MedComm: Oncol.*, 2024, **3**(1), e67.

79 X. Wei, G. Zhang, D. Ran, N. Krishnan, R. H. Fang, W. Gao, S. A. Spector and L. Zhang, T-cell-mimicking nanoparticles can neutralize HIV infectivity, *Adv. Mater.*, 2018, **30**(45), 1802233.

80 J. Varshosaz, S. Taymouri, E. Jafari, A. Jahanian-Najafabadi and A. Taheri, Formulation and characterization of cellulose acetate butyrate nanoparticles loaded with nevirapine for HIV treatment, *J. Drug Delivery Sci. Technol.*, 2018, **48**, 9–20.

81 R. F. Gonçalves, J. T. Martins, C. M. Duarte, A. A. Vicente and A. C. Pinheiro, Advances in nutraceutical delivery systems: From formulation design for bioavailability enhancement to efficacy and safety evaluation, *Trends Food Sci. Technol.*, 2018, **78**, 270–291.

82 H. Rostamabadi, S. R. Falsafi and S. M. Jafari, Starch-based nanocarriers as cutting-edge natural cargos for nutraceutical delivery, *Trends Food Sci. Technol.*, 2019, **88**, 397–415.

83 A. P. Ramos, M. A. Cruz, C. B. Tovani and P. Ciancaglini, Biomedical applications of nanotechnology, *Biophys. Rev.*, 2017, **9**(2), 79–89.

84 Z. U. Rahman, N. Wei, Z. Li, W. Sun and D. Wang, Preparation of hollow mesoporous silica nanospheres: Controllable template synthesis and their application in drug delivery, *New J. Chem.*, 2017, **41**(23), 14122–14129.

85 M. M. F. A. Baig, S. Khan, M. A. Naeem, G. J. Khan and M. T. Ansari, Vildagliptin loaded triangular DNA nanospheres coated with eudragit for oral delivery and better glycemic control in type 2 diabetes mellitus, *Biomed. Pharmacother.*, 2018, **97**, 1250–1258.

86 L. Sercombe, T. Veerati, F. Moheimani, S. Y. Wu, A. K. Sood and S. Hua, Advances and challenges of liposome assisted drug delivery, *Front. Pharmacol.*, 2015, **6**, 286.

87 M. Alavi and M. Hamidi, Passive and active targeting in cancer therapy by liposomes and lipid nanoparticles, *Drug Metab. Pers. Ther.*, 2019, **34**(1), 20180032.

88 J. Safari and Z. Zarnegar, Advanced drug delivery systems: Nanotechnology of health design A review, *J. Saudi Chem. Soc.*, 2014, **18**(2), 85–99.

89 X. Y. Sun, Q. Z. Gan and J. M. Ouyang, Size-dependent cellular uptake mechanism and cytotoxicity toward calcium oxalate on Vero cells, *Sci. Rep.*, 2017, **7**(1), 41949.

90 Y. Hui, X. Yi, F. Hou, D. Wibowo, F. Zhang, D. Zhao, H. Gao and C. X. Zhao, Role of nanoparticle mechanical properties in cancer drug delivery, *ACS Nano*, 2019, **13**(7), 7410–7424.

91 I. P. Mukha, A. M. Eremenko, N. P. Smirnova, A. I. Mikhienkova, G. I. Korchak, V. F. Gorchev and A. Y. Chunikhin, Antimicrobial activity of stable silver nanoparticles of a certain size, *Appl. Biochem. Microbiol.*, 2013, **49**, 199–206.

92 J. Panyam and V. Labhasetwar, Biodegradable nanoparticles for drug and gene delivery to cells and tissue, *Adv. Drug Delivery Rev.*, 2003, **55**(3), 329–347.

93 C. Buzea and I. Pacheco, Nanomaterial and nanoparticle: origin and activity, in *Nanoscience and Plant-Soil Systems*, 2017, pp. 71–112.

94 T. Lea, Caco-2 cell line, in *The Impact of Food Bioactives on Health: In vitro and Ex vivo Models*, 2015, pp. 103–111.

95 M. P. Desai, V. Labhasetwar, E. Walter, R. J. Levy and G. L. Amidon, The mechanism of uptake of biodegradable microparticles in Caco-2 cells is size dependent, *Pharm. Res.*, 1997, **14**, 1568–1573.

96 Y. Zare, Study of nanoparticles aggregation/agglomeration in polymer particulate nanocomposites by mechanical properties, *Composites, Part A*, 2016, **84**, 158–164.

97 W. Jiang, B. Y. Kim, J. T. Rutka and W. C. Chan, Nanoparticle-mediated cellular response is size-dependent, *Nat. Nanotechnol.*, 2008, **3**(3), 145–150.

98 A. Prokop and J. M. Davidson, Nanovehicular intracellular delivery systems, *J. Pharm. Sci.*, 2008, **97**(9), 3518–3590.

99 R. Ridolfo, S. Tavakoli, V. Junnuthula, D. S. Williams, A. Urtti and J. C. van Hest, Exploring the impact of morphology on the properties of biodegradable nanoparticles and their diffusion in complex biological medium, *Biomacromolecules*, 2020, **22**(1), 126–133.

100 M. C. Arno, M. Inam, A. C. Weems, Z. Li, A. L. Binch, C. I. Platt, S. M. Richardson, J. A. Hoyland, A. P. Dove and R. K. O'Reilly, Exploiting the role of nanoparticle shape in enhancing hydrogel adhesive and mechanical properties, *Nat. Commun.*, 2020, **11**(1), 1420.

101 Y. Liu, J. Hardie, X. Zhang and V. M. Rotello, Effects of engineered nanoparticles on the innate immune system, *Semin. Immunol.*, 2017, **34**, 25–32.

102 M. H. Bakalar, *et al.*, Size-dependent segregation controls macrophage phagocytosis of antibody- opsonized targets, *Cell*, 2018, **174**(1), 131–142.e13.



103 D. A. Hume, K. M. Irvine and C. Pridans, The mononuclear phagocyte system: the relationship between monocytes and macrophages, *Trends Immunol.*, 2019, **40**(2), 98–112.

104 S. B. Somvanshi, *et al.*, Hydrophobic to hydrophilic surface transformation of nano-scale zinc ferrite via oleic acid coating: magnetic hyperthermia study towards biomedical applications, *Ceram. Int.*, 2020, **46**(6), 7642–7653.

105 S. Y. Fam, *et al.*, Stealth coating of nanoparticles in drug-delivery systems, *Nanomaterials*, 2020, **10**(4), 787.

106 D. R. Perinelli, *et al.*, PEGylated poly(lactide) (PLA) and poly(lactic-co-glycolic acid)(PLGA) copolymers for the design of drug delivery systems, *J. Pharm. Invest.*, 2019, **49**(4), 443–458.

107 J. Hu, *et al.*, Poly(ethylene oxide)-based composite polymer electrolytes embedding with ionic bond modified nanoparticles for all-solid-state lithium-ion battery, *J. Membr. Sci.*, 2019, **575**, 200–208.

108 N. Wilkosz, *et al.*, Molecular insight into drug-loading capacity of PEG-PLGA nanoparticles for itraconazole, *J. Phys. Chem. B*, 2018, **122**(28), 7080–7090.

109 S. Ray, *et al.*, Polysorbate 80 coated crosslinked chitosan nanoparticles of ropinirole hydrochloride for brain targeting, *J. Drug Delivery Sci. Technol.*, 2018, **48**, 21–29.

110 G. L. Allotey-Babington, *et al.*, Cancer chemotherapy: Effect of poloxamer modified nanoparticles on cellular function, *J. Drug Delivery Sci. Technol.*, 2018, **47**, 181–192.

111 J. D. Clogston and A. K. Patri, Zeta potential measurement, in *Characterization of Nanoparticles Intended for Drug Delivery*, Springer, 2011, pp. 63–70.

112 E. Fröhlich, The role of surface charge in cellular uptake and cytotoxicity of medical nanoparticles, *Int. J. Nanomed.*, 2012, 5577–5591.

113 R. Xu, Progress in nanoparticles characterization: Sizing and zeta potential measurement, *Particuology*, 2008, **6**(2), 112–115.

114 M. C. Smith, *et al.*, Zeta potential: a case study of cationic, anionic, and neutral liposomes, *Anal. Bioanal. Chem.*, 2017, **409**(24), 5779–5787.

115 G. Yang, *et al.*, Bioinspired core-shell nanoparticles for hydrophobic drug delivery, *Angew. Chem.*, 2019, **131**(40), 14495–14502.

116 C. Buzea, I. Pacheco and K. Robbie, Nanomaterials and nanoparticles: sources and toxicity, *Biointerphases*, 2007, **90**(2), MR17–MR71, DOI: [10.1111/j.1365-2710.2007.01902.x](https://doi.org/10.1111/j.1365-2710.2007.01902.x).

117 Y. Liu, *et al.*, Stable polymer nanoparticles with exceptionally high drug loading by sequential nanoprecipitation, *Angew. Chem.*, 2020, **132**(12), 4750–4758.

118 S. Shen, *et al.*, High drug-loading nanomedicines: progress, current status, and prospects, *Int. J. Nanomed.*, 2017, **12**, 4085.

119 Y. Liu, *et al.*, Formulation of nanoparticles using mixing-induced nanoprecipitation for drug delivery, *Ind. Eng. Chem. Res.*, 2019, **59**(9), 4134–4149.

120 V. Kumar and R. K. Prud'Homme, Thermodynamic limits on drug loading in nanoparticle cores, *J. Pharm. Sci.*, 2008, **97**(11), 4904–4914.

121 S. Sepassi, *et al.*, Effect of polymer molecular weight on the production of drug nanoparticles, *J. Pharm. Sci.*, 2007, **96**(10), 2655–2666.

122 J. Wang and M. Windbergs, Influence of polymer composition and drug loading procedure on dual drug release from PLGA: PEG electrospun fibers, *Eur. J. Pharm. Sci.*, 2018, **124**, 71–79.

123 K. Kataoka, A. Harada and Y. Nagasaki, Block copolymer micelles for drug delivery: design, characterization and biological significance, *Adv. Drug Delivery Rev.*, 2012, **64**, 37–48.

124 W.-H. Lee, C.-Y. Loo and R. Rohanizadeh, Functionalizing the surface of hydroxyapatite drug carrier with carboxylic acid groups to modulate the loading and release of curcumin nanoparticles, *Mater. Sci. Eng., C*, 2019, **99**, 929–939.

125 Y. Liu, *et al.*, Development of High-Drug-Loading Nanoparticles, *ChemPlusChem*, 2020, **85**(9), 2143–2157.

126 G. Yang, *et al.*, Development of core-shell nanoparticle drug delivery systems based on biomimetic mineralization, *ChemBioChem*, 2020, **21**(20), 2871–2879.

127 L. Miao, *et al.*, Nanoparticles with precise ratiometric co-loading and co-delivery of gemcitabine monophosphate and cisplatin for treatment of bladder cancer, *Adv. Funct. Mater.*, 2014, **24**(42), 6601–6611.

128 N. Wang, *et al.*, Nanocarriers and their loading strategies, *Adv. Healthcare Mater.*, 2019, **8**(6), 1801002.

129 J. H. Lee and Y. Yeo, Controlled drug release from pharmaceutical nanocarriers, *Chem. Eng. Sci.*, 2015, **125**, 75–84.

130 C. E. Mora-Huertas, H. Fessi and A. Elaissari, Polymer-based nanocapsules for drug delivery, *Int. J. Pharm.*, 2010, **385**(1–2), 113–142.

131 G.-H. Son, B.-J. Lee and C.-W. Cho, Mechanisms of drug release from advanced drug formulations such as polymeric-based drug-delivery systems and lipid nanoparticles, *J. Pharm. Invest.*, 2017, **47**(4), 287–296.

132 S. Mura, J. Nicolas and P. Couvreur, Stimuli-responsive nanocarriers for drug delivery, *Nat. Mater.*, 2013, **12**(11), 991–1003.

133 R. Singh and J. W. Lillard Jr, Nanoparticle-based targeted drug delivery, *Exp. Mol. Pathol.*, 2009, **86**(3), 215–223.

134 H. P. James, *et al.*, Smart polymers for the controlled delivery of drugs—a concise overview, *Acta Pharm. Sin. B*, 2014, **4**(2), 120–127.

135 D. C. Costa, *et al.*, Laser ablation in liquid-assisted synthesis of three types of nanoparticles for enhanced antibacterial applications, *Int. J. Precis. Eng. Manuf. - Green Technol.*, 2025, 1–19.

136 R. Subedi and G. Guisbiers, Synthesis of ultrawide band gap TeO<sub>2</sub> nanoparticles by pulsed laser ablation in liquids: Top ablation versus bottom ablation, *ACS Omega*, 2024, **9**(24), 25832–25840.

137 T. T. N. Ho, T. Hirano, R. Narui, S. Imaoka, A. Takano, S. Miyasaka, E. Tanabe, E. L. Septiani, K. L. A. Cao and T. Ogi, Flame Spray Pyrolysis Achieves Size-Tunable Niobium-



doped Tin Oxide Nanoparticles for Improved Catalyst Performance in PEFCs, *ACS Appl. Energy Mater.*, 2025, **8**(7), 4640–4647.

138 H. Miao, *et al.*, One-step spray pyrolysis synthesis of ZnO/Ag hollow spheres for enhanced visible-light-driven antibacterial applications and wound healing, *Dalton Trans.*, 2025, **54**(6), 2574–2583.

139 T. Acsende, *et al.*, Enhancement of W Nanoparticles Synthesis by Injecting H<sub>2</sub> in a Magnetron Sputtering Gas Aggregation Cluster Source Operated in Ar, *Plasma Chem. Plasma Process.*, 2024, **44**(6), 2233–2246.

140 M. Protsak, *et al.*, One-step synthesis of photoluminescent nanofluids by direct loading of reactively sputtered cubic ZrN nanoparticles into organic liquids, *Nanoscale*, 2024, **16**(5), 2452–2465.

141 H. Fiedler, *et al.*, Room Temperature Ion Beam Synthesis of Ultra-Fine Molybdenum Carbide Nanoparticles: Toward a Scalable Fabrication Route for Earth-Abundant Electrodes, *Small*, 2024, **20**(39), 2304118.

142 V. Paperny, *et al.*, Enhancement of photoluminescence from rare-earth ions in fluoride crystals by ion-implanted silver nanoparticles, *J. Lumin.*, 2025, **279**, 121044.

143 A. N. Markov, *et al.*, Synthesis of Zinc Nanoparticles by the Gas Condensation Method in a Non-Contact Crucible and Their Physical-Chemical Characterization, *Nanomaterials*, 2024, **14**(2), 163.

144 K. Kollbek, *et al.*, Inert gas condensation made bimetallic FeCu nanoparticles–plasmonic response and magnetic ordering, *J. Mater. Chem. C*, 2024, **12**(7), 2593–2605.

145 M. Zarei, *et al.*, Fe-doped ZnO nanoparticles prepared by high energy ball milling with enhanced sonophotocatalytic performance, *Adv. Powder Technol.*, 2024, **35**(7), 104550.

146 G. T. Tractz, *et al.*, Enhancing photovoltaic performance through high-energy ball milling of Nb-doped TiO<sub>2</sub> nanoparticles, *MRS Commun.*, 2024, 1–7.

147 S. Dhital, *et al.*, Synthesis of manganese oxide nanoparticles using co-precipitation method and its antimicrobial activity, *Int. J. New Chem.*, 2024, **11**(3), 243–253.

148 M. Piran, M. Kharaziha and S. Sheibani, PVA-Assisted Synthesis of Cobalt Ferrite Nanoparticles for Biomedical Applications, *Ceram. Int.*, 2025, **02**, 049.

149 P. Nunocha, *et al.*, Efficient and novel synthesis of Nb-doped SrTiO<sub>3</sub> nanoparticles via microwave-assisted sol-gel auto-combustion, *Opt. Mater.*, 2025, **159**, 116665.

150 H. Nguyen, *et al.*, Electrochemical Synthesis of Silver Nanoparticles Using Camellia chrysanthia Flower Extract: Characteristics and Antibacterial Activity, *Colloid J.*, 2025, 1–10.

151 A. S. Joseph, *et al.*, Solvothermal synthesis of ruthenium-doped cobalt ferrite nanoparticles–A feasible approach to modify the magnetic properties and nonlinear optical absorption, *Mater. Sci. Semicond. Process.*, 2025, **188**, 109246.

152 S. Ahmad, *et al.*, Magnetic properties of different phases iron oxide nanoparticles prepared by micro emulsion-hydrothermal method, *Sci. Rep.*, 2025, **15**(1), 878.

153 A. Rajapantulu and R. Bandyopadhyaya, Role of Hydrazine and Size-Tuning Parameter in Gold Nanoparticle Synthesis by Water-in-Oil Microemulsion: Experiment and Simulation, *Langmuir*, 2025, **41**(12), 8049–8059.

154 R. Soomro, *et al.*, A novel plant-based approach for synthesis of iron oxide nanoparticles and cancer therapy, *Discover Chemistry*, 2025, **2**(1), 25.

155 R. Dhir, *et al.*, Plant-mediated synthesis of silver nanoparticles: unlocking their pharmacological potential—a comprehensive review, *Front. Bioeng. Biotechnol.*, 2024, **11**, 1324805.

156 M. Ebadi, *et al.*, A bio-inspired strategy for the synthesis of zinc oxide nanoparticles (ZnO NPs) using the cell extract of cyanobacterium *Nostoc* sp. EA03: from biological function to toxicity evaluation, *RSC Adv.*, 2019, **9**(41), 23508–23525.

157 N. Sani, B. Aminu and M. Mukhtar, Eco-friendly synthesis of silver nanoparticles using *Lactobacillus delbrueckii* subsp. *bulgaricus* isolated from kindrimo (locally fermented milk) in Kano State, Nigeria. *Bayero, J. Pure Appl. Sci.*, 2017, **10**(1), 481–488.

158 F. Ameen, Optimization of the synthesis of fungus-mediated bi-metallic Ag-Cu nanoparticles, *Appl. Sci.*, 2022, **12**(3), 1384.

159 K. Seku, *et al.*, Fungal-mediated synthesis of gold nanoparticles and their biological applications, in *Fungal Cell Factories for Sustainable Nanomaterials Productions and Agricultural Applications*, Elsevier, 2023, pp. 23–58.

160 A. A. K. Elrefaey, *et al.*, Algae-mediated biosynthesis of zinc oxide nanoparticles from *Cystoseira crinita* (Fucales; Sargassaceae) and its antimicrobial and antioxidant activities, *Egypt. J. Chem.*, 2022, **65**(4), 231–240.

161 M. Afrouz, *et al.*, Green synthesis of spermine coated iron nanoparticles and its effect on biochemical properties of *Rosmarinus officinalis*, *Sci. Rep.*, 2023, **13**(1), 775.

162 I. Hussain, *et al.*, Green synthesis of nanoparticles and its potential application, *Biotechnol. Lett.*, 2016, **38**, 545–560.

163 A. Gour and N. K. Jain, Advances in green synthesis of nanoparticles, *Artif. Cells, Nanomed., Biotechnol.*, 2019, **47**(1), 844–851.

164 M. Kim, *et al.*, Synthesis of nanoparticles by laser ablation: A review, *Kona Powder Part. J.*, 2017, **34**, 80–90.

165 N. Semaltianos, Nanoparticles by laser ablation, *Crit. Rev. Solid State Mater. Sci.*, 2010, **35**(2), 105–124.

166 A. S. Abd-Alrahman, R. A. Ismail and M. A. Mohammed, Synthesis of HgI<sub>2</sub> Nanoparticles and Nanorods by Laser Ablation in Liquid for Photodetector Applications: Effect of Laser Fluence, *J. Inorg. Organomet. Polym. Mater.*, 2022, 1–12.

167 A. B. Workie, H. S. Ningsih and S.-J. Shih, An comprehensive review on the spray pyrolysis technique: historical context, operational factors, classifications, and product applications, *J. Anal. Appl. Pyrolysis*, 2023, 105915.



168 M. A. Ismail, *et al.*, Synthesis and characterization of iron-doped TiO<sub>2</sub> nanoparticles using ferrocene from flame spray pyrolysis, *Catalysts*, 2021, **11**(4), 438.

169 W. Cheng, *et al.*, Synthesis of ZnS/CoS/CoS<sub>2</sub>@ N-doped carbon nanoparticles derived from metal-organic frameworks via spray pyrolysis as anode for lithium-ion battery, *J. Alloys Compd.*, 2020, **831**, 154607.

170 F. Wang, *et al.*, Magnetron sputtering enabled synthesis of nanostructured materials for electrochemical energy storage, *J. Mater. Chem. A*, 2020, **8**(39), 20260–20285.

171 T. Acсente, *et al.*, Tungsten Nanoparticles Produced by Magnetron Sputtering Gas Aggregation: Process Characterization and Particle Properties, *Prog. Fine Part. Plasmas*, 2020, 117.

172 M. Verma, K. P. Singh and A. Kumar, Reactive magnetron sputtering based synthesis of WO<sub>3</sub> nanoparticles and their use for the photocatalytic degradation of dyes, *Solid State Sci.*, 2020, **99**, 105847.

173 A. L. Stepanov, Synthesis of silver nanoparticles in dielectric matrix by ion implantation: A review, *Rev. Adv. Mater. Sci.*, 2010, **26**(1/2), 1–29.

174 R. Li, *et al.*, Plasmonic nanoparticles in dielectrics synthesized by ion beams: optical properties and photonic applications, *Adv. Opt. Mater.*, 2020, **8**(9), 1902087.

175 I. Lampé, *et al.*, Investigation of silver nanoparticles on titanium surface created by ion implantation technology, *Int. J. Nanomed.*, 2019, 4709–4721.

176 K. Zheng and P. S. Branicio, Synthesis of metallic glass nanoparticles by inert gas condensation, *Phys. Rev. Mater.*, 2020, **4**(7), 076001.

177 E. Pérez-Tijerina, *et al.*, Highly size-controlled synthesis of Au/Pd nanoparticles by inert-gas condensation, *Faraday Discuss.*, 2008, **138**, 353–362.

178 S. S. Mughal and S. M. Hassan, Comparative study of AgO nanoparticles synthesize via biological, chemical and physical methods: a review, *J. Mater. Synth. Process.*, 2022, **7**(2), 15–28.

179 G. Otis, M. Ejgenberg and Y. Mastai, Solvent-free mechanochemical synthesis of ZnO nanoparticles by high-energy ball milling of  $\varepsilon$ -Zn (OH) 2 crystals, *Nanomaterials*, 2021, **11**(1), 238.

180 P. Chin, *et al.*, Synthesis of FeS<sub>2</sub> and FeS nanoparticles by high-energy mechanical milling and mechanochemical processing, *J. Alloys Compd.*, 2005, **390**(1–2), 255–260.

181 D. Gao, *et al.*, Electrochemical synthesis of catalytic materials for energy catalysis, *Chin. J. Catal.*, 2022, **43**(4), 1001–1016.

182 V. Anand and V. C. Srivastava, Zinc oxide nanoparticles synthesis by electrochemical method: Optimization of parameters for maximization of productivity and characterization, *J. Alloys Compd.*, 2015, **636**, 288–292.

183 Y. Huo, *et al.*, Solvothermal synthesis and applications of micro/nano carbons: A review, *Chem. Eng. J.*, 2022, 138572.

184 M. A. Dar, *et al.*, Supercapacitor and magnetic properties of Fe doped SnS nanoparticles synthesized through solvothermal method, *J. Energy Storage*, 2022, **52**, 105034.

185 M. A. Malik, M. Y. Wani and M. A. Hashim, Microemulsion method: A novel route to synthesize organic and inorganic nanomaterials: 1st Nano Update, *Arabian J. Chem.*, 2012, **5**(4), 397–417.

186 J. N. Solanki and Z. V. P. Murthy, Controlled size silver nanoparticles synthesis with water-in-oil microemulsion method: a topical review, *Ind. Eng. Chem. Res.*, 2011, **50**(22), 12311–12323.

187 Z. Villagrán, *et al.*, Plant-based extracts as reducing, capping, and stabilizing agents for the green synthesis of inorganic nanoparticles, *Resources*, 2024, **13**(6), 70.

188 W. Wang, *et al.*, Biominerization: an opportunity and challenge of nanoparticle drug delivery systems for cancer therapy, *Adv. Healthcare Mater.*, 2020, **9**(22), 2001117.

189 W. Yang, *et al.*, Protein/peptide-templated biomimetic synthesis of inorganic nanoparticles for biomedical applications, *J. Mater. Chem. B*, 2017, **5**(3), 401–417.

190 X. Li, *et al.*, Biosynthesis of nanoparticles by microorganisms and their applications, *J. Nanomater.*, 2011, **2011**, 1–16.

191 R. Chaudhary, *et al.*, An overview of the algae-mediated biosynthesis of nanoparticles and their biomedical applications, *Biomolecules*, 2020, **10**(11), 1498.

192 N. Feroze, *et al.*, Fungal mediated synthesis of silver nanoparticles and evaluation of antibacterial activity, *Microsc. Res. Tech.*, 2020, **83**(1), 72–80.

193 M. Chen, S. Wang and B. Hu, Revealing the Formation of Well-Dispersed Polystyrene@ ZIF-8 Core–Shell Nanoparticles by Analytical Ultracentrifugation, *Langmuir*, 2020, **36**(29), 8589–8596.

194 A. Vaidya, *et al.*, Analytical characterization of heterogeneities in mRNA-lipid nanoparticles using sucrose density gradient ultracentrifugation, *Anal. Chem.*, 2024, **96**(14), 5570–5579.

195 S. H. Sajjadi, E. K. Goharshadi and H. Ahmadzadeh, Heat dissipation in slab gel electrophoresis: The effect of embedded TiO<sub>2</sub> nanoparticles on the thermal profiles, *J. Chromatogr. B: Anal. Technol. Biomed. Life Sci.*, 2019, **1118**, 63–69.

196 Y. Sun, *et al.*, DNA-Assisted Separation of Nanoparticles, *Small Methods*, 2024, 2401389.

197 L. Kuger, C. R. Arlt and M. Franzreb, Magnetic/flow controlled continuous size fractionation of magnetic nanoparticles using simulated moving bed chromatography, *Talanta*, 2022, **240**, 123160.

198 L. Pitkänen and A. M. Striegel, Size-exclusion chromatography of metal nanoparticles and quantum dots, *TrAC, Trends Anal. Chem.*, 2016, **80**, 311–320.

199 O. Milark, *et al.*, Design and Fabrication of 3D-Printed Lab-On-A-Chip Devices for Fiber-Based Optical Chromatography and Sorting, *Adv. Photonics Res.*, 2024, **5**(10), 2400011.

200 K. Yang, L. J. Huang, Y. X. Wang, Y. C. Du, Z. J. Zhang, Y. Wang, M. J. Kipper, L. A. Belfiore and J. G. Tang, Graphene oxide nanofiltration membranes containing silver nanoparticles: Tuning separation efficiency via nanoparticle size, *Nanomaterials*, 2020, **10**(3), 454.



201 E. Krieg, H. Weissman, E. Shirman, E. Shimoni and B. Rybtchinski, A recyclable supramolecular membrane for size-selective separation of nanoparticles, *Nat. Nanotechnol.*, 2011, **6**(3), 141–146.

202 X. Xu and H. Cölfen, Ultracentrifugation techniques for the ordering of nanoparticles, *Nanomaterials*, 2021, **11**(2), 333.

203 E. Karabudak, *et al.*, Simultaneous identification of spectral properties and sizes of multiple particles in solution with subnanometer resolution, *Angew. Chem., Int. Ed.*, 2016, **55**(39), 11770–11774.

204 R. P. Carney, *et al.*, Determination of nanoparticle size distribution together with density or molecular weight by 2D analytical ultracentrifugation, *Nat. Commun.*, 2011, **2**(1), 1–8.

205 H. Zhao, *et al.*, Overview of current methods in sedimentation velocity and sedimentation equilibrium analytical ultracentrifugation, *Curr. Protoc. Protein Sci.*, 2013, **71**(1), 20.12.1–20.12.49.

206 S. E. Wawra, *et al.*, Determination of the two-dimensional distributions of gold nanorods by multiwavelength analytical ultracentrifugation, *Nat. Commun.*, 2018, **9**(1), 4898.

207 M. Chen, S. Wang and B. Hu, Revealing the Formation of Well-Dispersed Polystyrene@ ZIF-8 Core–Shell Nanoparticles by Analytical Ultracentrifugation, *Langmuir*, 2020, **36**(29), 8589–8596.

208 T. Salafi, K. K. Zeming and Y. Zhang, Advancements in microfluidics for nanoparticle separation, *Lab Chip*, 2017, **17**(1), 11–33.

209 O. Akbulut, *et al.*, Separation of nanoparticles in aqueous multiphase systems through centrifugation, *Nano Lett.*, 2012, **12**(8), 4060–4064.

210 S. A. Claridge, *et al.*, Directed assembly of discrete gold nanoparticle groupings using branched DNA scaffolds, *Chem. Mater.*, 2005, **17**(7), 1628–1635.

211 X. Xu, *et al.*, Size and shape separation of gold nanoparticles with preparative gel electrophoresis, *J. Chromatogr. A*, 2007, **1167**(1), 35–41.

212 R. A. Sperling, *et al.*, Electrophoretic separation of nanoparticles with a discrete number of functional groups, *Adv. Funct. Mater.*, 2006, **16**(7), 943–948.

213 X. Zhu and T. G. Mason, Separating nanoparticles by surface charge group using pH-controlled passivated gel electrophoresis, *Soft Mater.*, 2016, **14**(3), 204–209.

214 D. Montizaan, *et al.*, Genome-wide forward genetic screening to identify receptors and proteins mediating nanoparticle uptake and intracellular processing, *Nat. Nanotechnol.*, 2024, **19**(7), 1022–1031.

215 M. Hanauer, *et al.*, Separation of nanoparticles by gel electrophoresis according to size and shape, *Nano Lett.*, 2007, **7**(9), 2881–2885.

216 A. Hlavacek, *et al.*, Large-scale purification of photon-upconversion nanoparticles by gel electrophoresis for analogue and digital bioassays, *Anal. Chem.*, 2018, **91**(2), 1241–1246.

217 H. Zorbas, *Bioanalytics: Methods on Molecular Biotechnology and Modern Biotechnology*, Wiley, New York, 2010.

218 L. Kuger, C.-R. Arlt and M. Franzreb, Magnetic/flow controlled continuous size fractionation of magnetic nanoparticles using simulated moving bed chromatography, *Talanta*, 2022, **240**, 123160.

219 L. Pitkänen and A. M. Striegel, Size-exclusion chromatography of metal nanoparticles and quantum dots, *TRAC, Trends Anal. Chem.*, 2016, **80**, 311–320.

220 H. Block, B. Maertens, A. Spriestersbach, N. Brinker, J. Kubicek, R. Fabis, J. Labahn and F. Schäfer, Immobilized-metal affinity chromatography (IMAC): a review, *Methods Enzymol.*, 2009, **463**, 439–473.

221 K. Yang, *et al.*, Graphene oxide nanofiltration membranes containing silver nanoparticles: Tuning separation efficiency via nanoparticle size, *Nanomaterials*, 2020, **10**(3), 454.

222 E. Krieg, *et al.*, A recyclable supramolecular membrane for size-selective separation of nanoparticles, *Nat. Nanotechnol.*, 2011, **6**(3), 141–146.

223 M. Samari, R. Heydari and F. Gholami, Nanofiltration membrane functionalized with CuxP nanoparticles: a promising approach for enhanced pesticide removal and long-term stability, *J. Cleaner Prod.*, 2024, **445**, 141352.

224 X. Tang, *et al.*, Theoretical and experimental study of high performance thin-film nanocomposite nanofiltration membranes by introducing calcium carbonate nanoparticles, *J. Membr. Sci.*, 2025, **713**, 123270.

225 G. M. Whitesides, The origins and the future of microfluidics, *Nature*, 2006, **442**(7101), 368–373.

226 M. I. Hajam and M. M. Khan, Microfluidics: a concise review of the history, principles, design, applications, and future outlook. *Biomaterials, Science*, 2024, **12**(2), 218–251.

227 S. Gimondi, *et al.*, Microfluidic mixing system for precise PLGA-PEG nanoparticles size control, *Nanomed.: Nanotechnol., Biol. Med.*, 2022, **40**, 102482.

228 T. Chen, Y. Peng, M. Qiu, C. Yi and Z. Xu, Recent Advances in Mixing-Induced Nanoprecipitation: From Creating Complex Nanostructures to Emerging Applications beyond Biomedicine, *Nanoscale*, 2023, **15**(8), 3594–3609.

229 J. Nette, P. D. Howes and A. J. deMello, Microfluidic Synthesis of Luminescent and Plasmonic Nanoparticles: Fast, Efficient, and Data-Rich, *Adv. Mater. Technol.*, 2020, **5**(7), 2000060.

230 N. Debnath, A. Kumar, T. Thundat and M. Sadrzadeh, Investigating fouling at the pore-scale using a microfluidic membrane mimic filtration system, *Sci. Rep.*, 2019, **9**(1), 10587.

231 V. M. Gun'ko, E. M. Pakhlov, O. V. Goncharuk, L. S. Andriyko, Y. M. Nychiporuk, D. Y. Balakin, D. Sternik and A. Derylo-Marczewska, Nanosilica modified by polydimethylsiloxane depolymerized and chemically bound to nanoparticles or physically bound to unmodified or modified surfaces: Structure and interfacial phenomena, *J. Colloid Interface Sci.*, 2018, **529**, 273–282.

232 X. Liu, *et al.*, Microfluidics chips fabrication techniques comparison, *Sci. Rep.*, 2024, **14**(1), 28793.



233 B. Amoyav and O. Benny, Controlled and tunable polymer particles' production using a single microfluidic device, *Appl. Nanosci.*, 2018, **8**(4), 905–914.

234 A. A. Volk, R. W. Epps and M. Abolhasani, Accelerated development of colloidal nanomaterials enabled by modular microfluidic reactors: toward autonomous robotic experimentation, *Adv. Mater.*, 2021, **33**(4), 2004495.

235 B. K. Gale, A. R. Jafek, C. J. Lambert, B. L. Goenner, H. Moghimifam, U. C. Nze and S. K. Kamarapu, A review of current methods in microfluidic device fabrication and future commercialization prospects, *Inventions*, 2018, **3**(3), 60.

236 J. Ahn, *et al.*, Microfluidics in nanoparticle drug delivery: From synthesis to pre-clinical screening, *Adv. Drug Delivery Rev.*, 2018, **128**, 29–53.

237 R. Riahi, *et al.*, Microfluidics for advanced drug delivery systems, *Curr. Opin. Chem. Eng.*, 2015, **7**, 101–112.

238 W. Raza, S.-B. Ma and K.-Y. Kim, Multi-objective optimizations of a serpentine micromixer with crossing channels at low and high Reynolds numbers, *Micromachines*, 2018, **9**(3), 110.

239 M. Rasouli, *et al.*, Multi-criteria optimization of curved and baffle-embedded micromixers for bio-applications, *Chem. Eng. Process.*, 2018, **132**, 175–186.

240 N.-T. Nguyen, *Micromixers: fundamentals, design and fabrication*, William Andrew, 2011.

241 S. I. Hamdallah, *et al.*, Microfluidics for pharmaceutical nanoparticle fabrication: The truth and the myth, *Int. J. Pharm.*, 2020, **584**, 119408.

242 J. D. Mello and A. D. Mello, FocusMicroscale reactors: nanoscale products, *Lab Chip*, 2004, **4**(2), 11N–15N.

243 A. J. Demello, Control and detection of chemical reactions in microfluidic systems, *Nature*, 2006, **442**(7101), 394–402.

244 Q. Feng, J. Sun and X. Jiang, Microfluidics-mediated assembly of functional nanoparticles for cancer-related pharmaceutical applications, *Nanoscale*, 2016, **8**(25), 12430–12443.

245 S. T. Sanjay, *et al.*, Recent advances of controlled drug delivery using microfluidic platforms, *Adv. Drug Delivery Rev.*, 2018, **128**, 3–28.

246 G. Antonelli, *et al.*, Integrating machine learning and biosensors in microfluidic devices: a review, *Biosens. Bioelectron.*, 2024, 116632.

247 J. Riordon, *et al.*, Deep learning with microfluidics for biotechnology, *Trends Biotechnol.*, 2019, **37**(3), 310–324.

248 X. Chen and H. Lv, Intelligent control of nanoparticle synthesis on microfluidic chips with machine learning, *NPG Asia Mater.*, 2022, **14**(1), 69.

249 C.-Y. Lee, C. L. Chang, Y. N. Wang and L. M. Fu, Microfluidic mixing: a review, *Int. J. Mol. Sci.*, 2011, **12**(5), 3263–3287.

250 W. Yao, *et al.*, Continuous synthesis of monodisperse polymer nanoparticles: New insights into the effects of experimental variables under controlled mixing conditions, *Chem. Eng. Sci.*, 2024, **288**, 119846.

251 S. M. Naghib and K. Mohammad-Jafari, Microfluidics-mediated Liposomal Nanoparticles for Cancer Therapy: Recent Developments on Advanced Devices and Technologies, *Curr. Top. Med. Chem.*, 2024, **24**(14), 1185–1211.

252 A. Hussain, *et al.*, Investigating hybrid nanoparticles for drug delivery in multi-stenosed catheterized arteries under magnetic field effects, *Sci. Rep.*, 2024, **14**(1), 1170.

253 A.-G. Niculescu, *et al.*, New 3D Vortex Microfluidic System Tested for Magnetic Core-Shell Fe<sub>3</sub>O<sub>4</sub>-SA Nanoparticle Synthesis, *Nanomaterials*, 2024, **14**(11), 902.

254 M. Abaee, S. Sohrabi and M. K. Moraveji, CFD assisted engineering of spiral microfluidic reactors for room temperature synthesis of ZnO nanoparticles, *Ceram. Int.*, 2024, **50**(18), 32613–32623.

255 D. J. Magdalene and D. Muthuselvam, Microfluidics assisted green synthesis of copper oxide nanoparticles from the aqueous leaf extract of Ipomoea quamoclit L. with its antimicrobial and antioxidant activity, *J. Herb. Med.*, 2024, **48**, 100940.

256 B. T. Ceccato, S. S. Vianna and L. G. de la Torre, Numerical and experimental investigation of chaotic advection and diffusion mixing effects in 3D multihelical microfluidics for liposome synthesis, *Chem. Eng. Sci.*, 2024, **295**, 120190.

257 D. Tomioka, *et al.*, Fabrication of oxygen-releasing dextran microgels by droplet-based microfluidic method, *RSC Adv.*, 2024, **14**(36), 26544–26555.

258 K. Ngocho, *et al.*, Synthetic Cells from Droplet-Based Microfluidics for Biosensing and Biomedical Applications, *Small*, 2024, **20**(33), 2400086.

259 H. Dortaj, *et al.*, Droplet-based microfluidics: an efficient high-throughput portable system for cell encapsulation, *J. Microencapsulation*, 2024, **41**(6), 479–501.

260 M. Lu, *et al.*, Microfluidic hydrodynamic focusing for synthesis of nanomaterials, *Nano Today*, 2016, **11**(6), 778–792.

261 X. Mao, S. C. S. Lin, C. Dong and T. J. Huang, Single-layer planar on-chip flow cytometer using microfluidic drifting based three-dimensional (3D) hydrodynamic focusing, *Lab Chip*, 2009, **9**(11), 1583–1589.

262 J.-M. Lim, *et al.*, Ultra-high throughput synthesis of nanoparticles with homogeneous size distribution using a coaxial turbulent jet mixer, *ACS Nano*, 2014, **8**(6), 6056–6065.

263 R. Baber, *et al.*, An engineering approach to synthesis of gold and silver nanoparticles by controlling hydrodynamics and mixing based on a coaxial flow reactor, *Nanoscale*, 2017, **9**(37), 14149–14161.

264 M. A. Daniele, *et al.*, 3D hydrodynamic focusing microfluidics for emerging sensing technologies, *Biosens. Bioelectron.*, 2015, **67**, 25–34.

265 G.-B. Lee, *et al.*, The hydrodynamic focusing effect inside rectangular microchannels, *J. Micromech. Microeng.*, 2006, **16**(5), 1024.

266 F. S. Majedi, *et al.*, Microfluidic synthesis of chitosan-based nanoparticles for fuel cell applications, *Chem. Commun.*, 2012, **48**(62), 7744–7746.



267 X. Mao, *et al.*, Single-layer planar on-chip flow cytometer using microfluidic drifting based three-dimensional (3D) hydrodynamic focusing, *Lab Chip*, 2009, **9**(11), 1583–1589.

268 X. Mao, J. R. Waldeisen and T. J. Huang, Microfluidic drifting—implementing three-dimensional hydrodynamic focusing with a single-layer planar microfluidic device, *Lab Chip*, 2007, **7**(10), 1260–1262.

269 T. Baby, *et al.*, Fundamental studies on throughput capacities of hydrodynamic flow-focusing microfluidics for producing monodisperse polymer nanoparticles, *Chem. Eng. Sci.*, 2017, **169**, 128–139.

270 F. Heshmatnezhad, *et al.*, Production of doxorubicin-loaded PCL nanoparticles through a flow-focusing microfluidic device: encapsulation efficacy and drug release, *Soft Matter*, 2021, **17**(47), 10675–10682.

271 A. D. Stroock, *et al.*, Chaotic mixer for microchannels, *Science*, 2002, **295**(5555), 647–651.

272 H. Amini, W. Lee and D. Di Carlo, Inertial microfluidic physics, *Lab Chip*, 2014, **14**(15), 2739–2761.

273 Y. Kim, *et al.*, Mass production and size control of lipid-polymer hybrid nanoparticles through controlled microvortices, *Nano Lett.*, 2012, **12**(7), 3587–3591.

274 H. Ahmed, S. Ramesan, L. Lee, A. R. Rezk and L. Y. Yeo, On-chip generation of vortical flows for microfluidic centrifugation, *Small*, 2020, **16**(9), 1903605.

275 Y. Li, C. Liu, X. Bai, F. Tian, G. Hu and J. Sun, Enantiomeric Microvortex-Enabled Supramolecular Sensing of Racemic Amino Acids by Using Achiral Building Blocks, *Angew. Chem., Int. Ed.*, 2020, **59**(9), 3486–3490.

276 D. Liu, *et al.*, A versatile and robust microfluidic platform toward high throughput synthesis of homogeneous nanoparticles with tunable properties, *Adv. Mater.*, 2015, **27**(14), 2298–2304.

277 G. Karniadakis, A. Beskok and N. Aluru, Mixers and chaotic advection, *Microflows and Nanoflows: Fundamentals and Simulation*, 2005, pp. 343–363.

278 X. Zhang, *et al.*, Continuous high-flux synthesis of gold nanoparticles with controllable sizes: a simple microfluidic system, *Appl. Nanosci.*, 2020, **10**, 661–669.

279 W. Fan, F. Zhao, M. Chen, J. Li and X. Guo, An efficient microreactor with continuous serially connected micromixers for the synthesis of superparamagnetic magnetite nanoparticles, *Chin. J. Chem. Eng.*, 2023, **59**, 85–91.

280 D. R. Kumar, B. Prasad and A. Kulkarni, Segmented flow synthesis of Ag nanoparticles in spiral microreactor: Role of continuous and dispersed phase, *Chem. Eng. J.*, 2012, **192**, 357–368.

281 R. T. Tsai and C. Y. Wu, An efficient micromixer based on multidirectional vortices due to baffles and channel curvature, *Biomicrofluidics*, 2011, **5**(1), 014103.

282 C. K. Chung, T. R. Shih, C. K. Chang, C. W. Lai and B. H. Wu, Design and experiments of a short-mixing-length baffled microreactor and its application to microfluidic synthesis of nanoparticles, *Chem. Eng. J.*, 2011, **168**(2), 790–798.

283 J. Sun, Y. Xianyu, M. Li, W. Liu, L. Zhang, D. Liu, C. Liu, G. Hu and X. Jiang, A microfluidic origami chip for synthesis of functionalized polymeric nanoparticles, *Nanoscale*, 2013, **5**(12), 5262–5265.

284 B. Q. Ta, H. Le Thanh, T. Dong, T. N. Thoi and F. Karlsen, Geometric effects on mixing performance in a novel passive micromixer with trapezoidal-zigzag channels, *J. Micromech. Microeng.*, 2015, **25**(9), 094004.

285 A. Bokare, A. Takami, J. H. Kim, A. Dong, A. Chen, R. Valerio, S. Gunn and F. Erogbogbo, Herringbone-patterned 3D-printed devices as alternatives to microfluidics for reproducible production of lipid polymer hybrid nanoparticles, *ACS Omega*, 2019, **4**(3), 4650–4657.

286 W. W. Liu and Y. Zhu, Development and application of analytical detection techniques for droplet-based microfluidics—A review, *Anal. Chim. Acta*, 2020, **1113**, 66–84.

287 Y. Zhang, H. F. Chan and K. W. Leong, Advanced materials and processing for drug delivery: the past and the future, *Adv. Drug Delivery Rev.*, 2013, **65**(1), 104–120.

288 I. Shestopalov, J. D. Tice and R. F. Ismagilov, Multi-step synthesis of nanoparticles performed on millisecond time scale in a microfluidic droplet-based system, *Lab Chip*, 2004, **4**(4), 316–321.

289 I.-L. Ngo, S. Woo Joo and C. Byon, Effects of junction angle and viscosity ratio on droplet formation in microfluidic cross-junction, *J. Fluids Eng.*, 2016, **138**(5), 051202.

290 R. Baber, L. Mazzei, N. T. Thanh and A. Gavrilidis, Synthesis of silver nanoparticles in a microfluidic coaxial flow reactor, *RSC Adv.*, 2015, **5**(116), 95585–95591.

291 S. Sohrabi and M. K. Moraveji, Droplet microfluidics: Fundamentals and its advanced applications, *RSC Adv.*, 2020, **10**(46), 27560–27574.

292 Y. Ding, P. D. Howes and A. J. deMello, Recent advances in droplet microfluidics, *Anal. Chem.*, 2019, **92**(1), 132–149.

293 M. V. Bandulasena, G. T. Vladisavljević and B. Benyahia, Droplet-based microfluidic method for robust preparation of gold nanoparticles in axisymmetric flow focusing device, *Chem. Eng. Sci.*, 2019, **195**, 657–664.

294 M. Karimian, K. Dashtian and R. Zare-Dorabei, Microfluidic chip and chiroptical gold nanoparticle-based colorimetric sensor for enantioselective detection of L-tryptophan, *Talanta*, 2024, **266**, 125138.

295 G. He, *et al.*, Microfluidic synthesis of CuH nanoparticles for antitumor therapy through hydrogen-enhanced apoptosis and cuproptosis, *ACS Nano*, 2024, **18**(12), 9031–9042.

296 A. Azmeer, *et al.*, Finger-operated pumping platform for microfluidic preparation of nanoparticles, *Microfluid. Nanofluid.*, 2024, **28**(7), 43.

297 T. N. Banavathi, M. K. Sivakumar, A. Balapure, S. Dudala, S. K. Dubey and S. Goel, Microfluidic Microreactor Device with Integrated Heaters for Temperature Assisted Synthesis of Gold Nanoparticles and Alkene, *IEEE Open J. Nanotechnol.*, 2024(5), 134–140.

298 H. Liu, X. Lan, Y. Yin, X. Wang, X. Chen, J. Zhou, K. Chen and X. Zhang, Green Synthesis and Durable Antibacterial AgNP-Loaded Alginate Fibers Enabled by Microfluidic



Technology Coupled with Ultraviolet/Thermal Fields, *ACS Appl. Polym. Mater.*, 2025, **7**(8), 5259–5270.

299 L. Wang, *et al.*, G-Quadruplex DNAzyme-Based Biocatalysis Combined with an Intelligent Electromagnetic-Actuated Microfluidic Chip for Tetracycline Detection, *J. Agric. Food Chem.*, 2024, **73**(2), 1598–1607.

300 Y.-T. Kang, *et al.*, Chiroptical detection and mutation analysis of cancer-associated extracellular vesicles using microfluidics with oriented chiral nanoparticles, *Matter*, 2024, **7**(12), 4373–4389.

301 K. Curtin, T. Godary and P. Li, Synthesis of tunable gold nanostars via 3D-printed microfluidic device with vibrating sharp-tip acoustic mixing, *Microfluid. Nanofluid.*, 2023, **27**(11), 77.

302 A. P. Vardin, F. Aksoy and G. Yesiloz, A Novel Acoustic Modulation of Oscillating Thin Elastic Membrane for Enhanced Streaming in Microfluidics and Nanoscale Liposome Production, *Small*, 2024, **20**(48), 2403463.

303 Z. Saifi, *et al.*, Formulation approaches and pharmaceutical applications of chitosan and thiolated chitosan nanoparticles, *J. Carbohydr. Chem.*, 2025, 1–30.

304 S. Karmakar, *et al.*, Nanoparticle Deposition Techniques for Silica Nanoparticles: Synthesis, Electrophoretic Deposition, and Optimization-A review, *arXiv*, 2025, preprint, arXiv:2503.22593, DOI: [10.48550/arXiv/2503.22593](https://doi.org/10.48550/arXiv/2503.22593).

305 O. Strohmeier, *et al.*, Centrifugal microfluidic platforms: advanced unit operations and applications, *Chem. Soc. Rev.*, 2015, **44**(17), 6187–6229.

306 H. Van Nguyen, *et al.*, Serially diluting centrifugal microfluidics for high-throughput gold nanoparticle synthesis using an automated and portable workstation, *Chem. Eng. J.*, 2023, **452**, 139044.

307 H. Van Nguyen, *et al.*, Centrifugal microfluidic device for the high-throughput synthesis of Pd@ AuPt core-shell nanoparticles to evaluate the performance of hydrogen peroxide generation, *Lab Chip*, 2020, **20**(18), 3293–3301.

308 A. A. Deshmukh, D. Liepmann and A. P. Pisano, Continuous micromixer with pulsatile micropumps, in *Technical Digest of the IEEE Solid State Sensor and Actuator Workshop*, Hilton Head Island, SC, 2000.

309 J. W. Wu, H. M. Xia, Y. Y. Zhang, S. F. Zhao, P. Zhu and Z. P. Wang, An efficient micromixer combining oscillatory flow and divergent circular chambers, *Microsyst. Technol.*, 2019, **25**(7), 2741–2750.

310 W.-B. Lee, *et al.*, Biomedical microdevices synthesis of iron oxide nanoparticles using a microfluidic system, *Biomed. Microdevices*, 2009, **11**, 161–171.

311 K. Sugano, *et al.*, Mixing speed-controlled gold nanoparticle synthesis with pulsed mixing microfluidic system, *Microfluid. Nanofluid.*, 2010, **9**, 1165–1174.

312 S. M. Recktenwald, C. Wagner and T. John, Optimizing pressure-driven pulsatile flows in microfluidic devices, *Lab Chip*, 2021, **21**(13), 2605–2613.

313 Z. Li and S. J. Kim, Pulsatile micromixing using water-head-driven microfluidic oscillators, *Chem. Eng. J.*, 2017, **313**, 1364–1369.

314 G. Kunti, A. Bhattacharya and S. Chakraborty, Electrothermally actuated moving contact line dynamics over chemically patterned surfaces with resistive heaters, *Phys. Fluids*, 2018, **30**(6), 2004.

315 J.-H. Tsai, L. J. S. Lin and A. A. Physical, Active microfluidic mixer and gas bubble filter driven by thermal bubble micropump, *Sens. Actuators, A*, 2002, **97**, 665–671.

316 H. Mao, T. Yang and P. S. Cremer, A microfluidic device with a linear temperature gradient for parallel and combinatorial measurements, *J. Am. Chem. Soc.*, 2002, **124**(16), 4432–4435.

317 H. Sun, *et al.*, Three-fluid sequential micromixing-assisted nanoparticle synthesis utilizing alternating current electrothermal flow, *Ind. Eng. Chem. Res.*, 2020, **59**(27), 12514–12524.

318 H. Lv and X. Chen, New insights into the mechanism of fluid mixing in the micromixer based on alternating current electric heating with film heaters, *Int. J. Heat Mass Transfer*, 2021, **181**, 121902.

319 S. Srikanth, S. Dudala, U. S. Jayapiriy, J. M. Mohan, S. Raut, S. K. Dubey, I. Ishii, A. Javed and S. Goel, Droplet-based lab-on-chip platform integrated with laser ablated graphene heaters to synthesize gold nanoparticles for electrochemical sensing and fuel cell applications, *Sci. Rep.*, 2021, **11**(1), 9750.

320 H. Tan, Numerical study of a bubble driven micromixer based on thermal inkjet technology, *Phys. Fluids*, 2019, **31**(6), 062006.

321 J. Wu, W. Cao, W. Wen, D. C. Chang and P. Sheng, Polydimethylsiloxane microfluidic chip with integrated microheater and thermal sensor, *Biomicrofluidics*, 2009, **3**(1), 012005.

322 L. Huang, *et al.*, Rational Design of 3D-Printed Microfluidic Chips for One-Step Production of Silver Nanofluids in Thermal Management of Power Electronic Chips, *ACS Appl. Mater. Interfaces*, 2025, **17**(15), 23277–23285.

323 E. Weaver, *et al.*, The manufacturing of 3D-printed microfluidic chips to analyse the effect upon particle size during the synthesis of lipid nanoparticles, *J. Pharm. Pharmacol.*, 2023, **75**(2), 245–252.

324 S. Dembski, *et al.*, Establishing and testing a robot-based platform to enable the automated production of nanoparticles in a flexible and modular way, *Sci. Rep.*, 2023, **13**(1), 11440.

325 M. A. Nestrup, *et al.*, A versatile, low-cost modular microfluidic system to prepare poly (lactic-co-glycolic acid) nanoparticles with encapsulated protein, *Pharm. Res.*, 2024, **41**(12), 2347–2361.

326 A. Kouhkord, *et al.*, Controllable microfluidic system through intelligent framework: Data-driven modeling, machine learning energy analysis, comparative multiobjective optimization, and experimental study, *Ind. Eng. Chem. Res.*, 2024, **63**(30), 13326–13344.

327 S. Mihandoost, *et al.*, A Generative Adversarial Network Approach to Predict Nanoparticle Size in Microfluidics, *ACS Biomater. Sci. Eng.*, 2024, **11**(1), 268–279.



328 S. Gao, *et al.*, Artificial Intelligence Enhanced Microfluidic System for Multiplexed Point-of-care-testing of Biological Thiols, *Talanta*, 2025, 127619.

329 M. Ballard, *et al.*, Orbiting magnetic microbeads enable rapid microfluidic mixing, *Microfluid. Nanofluid.*, 2016, **20**(6), 1–13.

330 A. N. Surendran and R. Zhou, Active High-Throughput Micromixer Using Injected Magnetic Mixture Underneath Microfluidic Channel, in *International Conference on Nanochannels, Microchannels, and Minichannels*, American Society of Mechanical Engineers, 2020, vol. 83693, p. V001T01A001.

331 J. Sun, Z. Shi, M. Li, J. Sha, M. Zhong, S. Chen, X. Liu and S. Jia, Numerical and experimental investigation of a magnetic micromixer under microwires and uniform magnetic field, *J. Magn. Magn. Mater.*, 2022, **551**, 169141.

332 D. Bahrami, A. A. Nadooshan and M. Bayareh, Effect of non-uniform magnetic field on mixing index of a sinusoidal micromixer, *Korean J. Chem. Eng.*, 2022, 1–12.

333 A. Dehghan, A. Gholizadeh, M. Navidbakhsh, H. Sadeghi and E. Pishbin, Integrated microfluidic system for efficient DNA extraction using on-disk magnetic stirrer micromixer, *Sens. Actuators, B*, 2022, **351**, 130919.

334 Y. A. Wu, B. Panigrahi, Y. H. Lu and C. Y. Chen, An integrated artificial cilia based microfluidic device for micropumping and micromixing applications, *Micromachines*, 2017, **8**(9), 260.

335 N. Banka, Y. L. Ng and S. Devasia, Individually controllable magnetic cilia: Mixing application, *J. Med. Devices*, 2017, **11**(3), 031003.

336 B. Panigrahi, V. Sahadevan and C.-Y. Chen, Shape-programmable artificial cilia for microfluidics, *iScience*, 2021, **24**(12), 103367.

337 N. Veldurthi, P. Ghoderao, S. Sahare, V. Kumar, D. Bodas, A. Kulkarni and T. Bhave, Magnetically active micromixer assisted synthesis of drug nanocomplexes exhibiting strong bactericidal potential, *Mater. Sci. Eng., C*, 2016, **68**, 455–464.

338 J. S. Bach and H. Bruus, Suppression of acoustic streaming in shape-optimized channels, *Phys. Rev. Lett.*, 2020, **124**(21), 214501.

339 P. Marmottant, J. P. Raven, H. J. G. E. Gardeniers, J. G. Bomer and S. Hilgenfeldt, Microfluidics with ultrasound-driven bubbles, *J. Fluid Mech.*, 2006, **568**, 109–118.

340 A. Ozcelik, J. Rufo, F. Guo, Y. Gu, P. Li, J. Lata and T. J. Huang, Acoustic tweezers for the life sciences, *Nat. Methods*, 2018, **15**(12), 1021–1028.

341 P. Li, Z. Mao, Z. Peng, L. Zhou, Y. Chen, P. H. Huang, C. I. Truica, J. J. Drabick, W. S. El-Deiry, M. Dao and S. Suresh, Acoustic separation of circulating tumor cells, *Proc. Natl. Acad. Sci. U. S. A.*, 2015, **112**(16), 4970–4975.

342 R. H. Liu, J. Yang, M. Z. Pindera, M. Athavale and P. Grodzinski, Bubble-induced acoustic micromixing, *Lab Chip*, 2002, **2**(3), 151–157.

343 A. Hashmi, G. Yu, M. Reilly-Collette, G. Heiman and J. Xu, Oscillating bubbles: a versatile tool for lab on a chip applications, *Lab Chip*, 2012, **12**(21), 4216–4227.

344 D. Ahmed, C. Y. Chan, S. C. S. Lin, H. S. Muddana, N. Nama, S. J. Benkovic and T. J. Huang, Tunable, pulsatile chemical gradient generation via acoustically driven oscillating bubbles, *Lab Chip*, 2013, **13**(3), 328–331.

345 P.-H. Huang, N. Nama, Z. Mao, P. Li, J. Rufo, Y. Chen, Y. Xie, C. H. Wei, L. Wang and T. J. Huang, A reliable and programmable acoustofluidic pump powered by oscillating sharp-edge structures, *Lab Chip*, 2014, **14**(22), 4319–4323.

346 M. R. Rasouli and M. Tabrizian, An ultra-rapid acoustic micromixer for synthesis of organic nanoparticles, *Lab Chip*, 2019, **19**(19), 3316–3325.

347 N. H. A. Le, *et al.*, Ultrafast star-shaped acoustic micromixer for high throughput nanoparticle synthesis, *Lab Chip*, 2020, **20**(3), 582–591.

348 P. H. Huang, *et al.*, Acoustofluidic synthesis of particulate nanomaterials, *Adv. Sci.*, 2019, **6**(19), 1900913.

349 H.-S. Kim, H.-O. Kim and Y.-J. Kim, Effect of electrode configurations on the performance of electro-hydrodynamic micromixer, in *International Conference on Nanochannels, Microchannels, and Minichannels*, American Society of Mechanical Engineers, 2018, vol. 51197, p. V001T02A005.

350 S. Rashidi, H. Bafekr, M. S. Valipour and J. A. Esfahani, A review on the application, simulation, and experiment of the electrokinetic mixers, *Chem. Eng. Process.*, 2018, **126**, 108–122.

351 X. Ou, P. Chen, X. Huang, S. Li and B. F. Liu, Microfluidic chip electrophoresis for biochemical analysis, *J. Sep. Sci.*, 2020, **43**(1), 258–270.

352 A. Alizadeh, W. L. Hsu, M. Wang and H. Daiguji, Electroosmotic flow: From microfluidics to nanofluidics, *Electrophoresis*, 2021, **42**(7–8), 834–868.

353 H. Zhang, H. Chang and P. J. M. Neuzil, DEP-on-a-chip: Dielectrophoresis applied to microfluidic platforms, *Micromachines*, 2019, **10**(6), 423.

354 J. J. Huang, Y. J. Lo, C. M. Hsieh, U. Lei, C. I. Li and C. W. Huang, An electro-thermal micro mixer, in *2011 6th IEEE International Conference on Nano/Micro Engineered and Molecular Systems (MEMS)*, IEEE, 2011.

355 T. Zhou, H. Wang, L. Shi, Z. Liu and S. W. Joo, An enhanced electroosmotic micromixer with an efficient asymmetric lateral structure, *Micromachines*, 2016, **7**(12), 218.

356 P. Modarres and M. Tabrizian, Nanoparticle Synthesis Using an Electrohydrodynamic Micromixer, in *2020 IEEE 33rd International Conference on Micro Electro Mechanical Systems (MEMS)*, IEEE, 2020, pp. 1068–1070.

357 Y. Daghighi and D. Li, Numerical study of a novel induced-charge electrokinetic micro-mixer, *Anal. Chim. Acta*, 2013, **763**, 28–37.

358 J. E. Ortiz-Castillo, M. Vazquez-Pinon, S. O. Martinez-Chapa and V. H. Perez-Gonzalez, A reactor-on-a-chip for cost-effective synthesis of gold nanoparticles, *Mater. Today: Proc.*, 2020, **48**, 10–15.

359 K. Rahali, A. G. Tabriz and D. Douroumis, The effect of 3D printed microfluidic array designs on the preparation of liposome nanoparticles, *J. Drug Delivery Sci. Technol.*, 2024, **94**, 105411.



360 N. V. Egil, *et al.*, High-throughput screening of gold nanoparticle synthesis parameters in droplet microfluidics, *Mendeleev Commun.*, 2024, **34**(6), 783–785.

361 G. Gkogkos, *et al.*, A compact 3D printed magnetically stirred tank reactor cascade coupled with a free impinging jet for continuous production of colloidal nanoparticles, *Chem. Eng. Sci.*, 2024, **294**, 120081.

362 I. Arduino, *et al.*, The manufacturing and characterization of pentamidine-loaded poly (lactic-co-glycolic acid) nanoparticles produced by microfluidic method, *J. Drug Delivery Sci. Technol.*, 2024, **100**, 106063.

363 D. Zhang, *et al.*, Microfluidic Technology: A New Strategy for Controllable Synthesis of Metal Nanomaterials, *ChemElectroChem*, 2025, e202400666.

364 T. P. Rosalba, *et al.*, A modular flow process intensification towards lipid peptoids nano assembly formation, *J. Flow Chem.*, 2024, **14**(4), 677–689.

365 I. S. Pires, *et al.*, High-Throughput Microfluidic-Mediated Assembly of Layer-By-Layer Nanoparticles, *Adv. Funct. Mater.*, 2025, 2503965.

366 B. Huwaimel and S. Alqarni, Design of Poly (lactic-co-glycolic acid) nanoparticles in drug delivery by artificial intelligence methods to find the conditions of nanoparticles synthesis, *Chemom. Intell. Lab. Syst.*, 2025, 105335.

367 K. Nathanael, S. Cheng, N. M. Kovalchuk, R. Arcucci and M. J. Simmons, Optimisation of Microfluidic Synthesis of Silver Nanoparticles via Data-driven Inverse Modelling, *Chem. Eng. Res. Des.*, 2025, **216**, 523–530.

368 Y. Yuan, Y. Li, G. Li, L. Lei, X. Huang, M. Li and Y. Yao, Intelligent Design of Lipid Nanoparticles for Enhanced Gene Therapeutics, *Mol. Pharmaceutics*, 2025, **22**(3), 1142–1159.

369 S. Orsini, M. Lauricella, A. Montessori, A. Tiribocchi, M. Durve, S. Succi, L. Persano, A. Camposeo and D. Pisignano, 3D printing and artificial intelligence tools for droplet microfluidics: Advances in the generation and analysis of emulsions, *Appl. Phys. Rev.*, 2025, **12**(1), 011306.

370 S. Rezvantalab, S. Mihandoost and M. Rezaiee, Machine learning assisted exploration of the influential parameters on the PLGA nanoparticles, *Sci. Rep.*, 2024, **14**(1), 1114.

371 N. Seegobin, *et al.*, Optimising the production of PLGA nanoparticles by combining design of experiment and machine learning, *Int. J. Pharm.*, 2024, **667**, 124905.

372 J. Atencia, *et al.*, Magnetic connectors for microfluidic applications, *Lab Chip*, 2010, **10**(2), 246–249.

373 Q. Xu, J. C. C. Lo and S.-W. R. Lee, Directly printed hollow connectors for microfluidic interconnection with UV-assisted coaxial 3D printing, *Appl. Sci.*, 2020, **10**(10), 3384.

374 M. Alvarez-Amador, A. Salimov and E. Brouzes, Universal and Versatile Magnetic Connectors for Microfluidic Devices, *Micromachines*, 2024, **15**(6), 803.

375 Z. Shi, H. Wang and Y. Zhang, A fast and plug-and-play mechanical connector for microfluidic chips, *J. Phys.: Conf. Ser.*, 2024, **2740**, 012004.

376 X. Liu and H. Meng, Consideration for the scale-up manufacture of nanotherapeutics—A critical step for technology transfer, *View*, 2021, **2**(5), 20200190.

377 L. Gomez, *et al.*, Scaled-up production of plasmonic nanoparticles using microfluidics: from metal precursors to functionalized and sterilized nanoparticles, *Lab Chip*, 2014, **14**(2), 325–332.

378 S. J. Shepherd, *et al.*, Scalable mRNA and siRNA lipid nanoparticle production using a parallelized microfluidic device, *Nano Lett.*, 2021, **21**(13), 5671–5680.

